

1 Journal: Soil Biology and Biochemistry  
2 Special Issue: Advances in Modelling Soil Microbial Dynamics

3

#### 4 **Aligning theoretical and empirical representations of soil carbon-to-nitrogen 5 stoichiometry with process-based terrestrial biogeochemistry models**

6 Katherine S. Rocci<sup>1, 2</sup>, Cory C. Cleveland<sup>3</sup>, Brooke A. Eastman<sup>4</sup>, Katerina Georgiou<sup>5</sup>, A. Stuart Grandy<sup>6, 7</sup>,  
7 Melannie D. Hartman<sup>8</sup>, Emma Hauser<sup>3</sup>, Hannah Holland-Moritz<sup>6, 7</sup>, Emily Kyker-Snowman<sup>9</sup>, Derek  
8 Pierson<sup>10</sup>, Peter B. Reich<sup>2, 11</sup>, Else P. Schlerman<sup>6, 7</sup>, William R. Wieder<sup>1, 12</sup>

9

10 <sup>1</sup>Institute of Arctic and Alpine Research, University of Colorado, Boulder, CO; <sup>2</sup>Institute for Global Change  
11 Biology, University of Michigan, Ann Arbor, MI; <sup>3</sup>Department of Ecosystem and Conservation Sciences,  
12 W.A. Franke College of Forestry and Conservation, University of Montana, Missoula, MT; <sup>4</sup>Department of  
13 Biology, West Virginia University, Morgantown, WV; <sup>5</sup>Physical and Life Sciences Directorate, Lawrence  
14 Livermore National Laboratory, Livermore, CA; <sup>6</sup>Department of Natural Resources and the Environment,  
15 University of New Hampshire, Durham, NH; <sup>7</sup>Center of Soil Biogeochemistry and Microbial Ecology  
16 (Soil BioME), University of New Hampshire, Durham NH; <sup>8</sup>Natural Resource Ecology Laboratory,  
17 Colorado State University, Fort Collins, CO; <sup>9</sup>Carbon Direct, New York, NY; <sup>10</sup>Rocky Mountain Research  
18 Station, United States Forest Service, Boise, ID; <sup>11</sup>Department of Forest Resources, University of  
19 Minnesota, St. Paul, MN; <sup>12</sup>Climate and Global Dynamics Laboratory, National Center for Atmospheric  
20 Research, Boulder, CO

## 21 **Abstract**

22 Soil carbon-nitrogen (C:N) stoichiometry acts as a control over decomposition and soil  
23 organic matter formation and loss, making it a key soil property for understanding ecosystem  
24 dynamics and projected ecosystems responses to global environmental change. However, the  
25 controls of soil C:N and how they respond to increasing pressures from global change agents  
26 are not fully understood. The “foundational” controls on soil C:N, namely plant and microbial  
27 C:N, have been used to predict soil C:N, but fail to accurately simulate all ecosystems and may  
28 be insufficient for predictions under global environmental change. We present an “emerging”  
29 representation of controls of soil C:N that includes plant-microbe-mineral feedbacks that have  
30 been shown to regulate soil C:N. We argue that including representation of these emerging  
31 drivers in process-based terrestrial biogeochemistry models, which include biological N fixation,  
32 mycorrhizae, priming, root exudation of organic acids, and mineralogy (including soil texture,  
33 mineral composition, and aggregation), will improve mechanistic representation of soil C:N and

34 associated processes. Such improvements will produce models that will better simulate a  
35 variety of ecological states and predict soil C:N when global changes modify plant-microbe-  
36 mineral interactions. Here, we align our empirical understanding of controls of soil C:N with  
37 those controls represented in models, identifying contexts where emerging drivers might be  
38 particularly important to represent (e.g., priming and root exudation in nutrient-limited  
39 conditions) and areas of future work. Additionally, we show that implementing emerging drivers  
40 of soil C:N results in different simulated outcomes at steady state and in response to elevated  
41 atmospheric CO<sub>2</sub>. Our review and preliminary simulations support the need to incorporate  
42 emerging drivers of soil C:N into process-based terrestrial biogeochemistry models, allowing for  
43 both theoretical exploration of mechanisms and potentially more accurate predictions of land  
44 biogeochemical responses to global change.

## 45 1. Introduction

46 Ecological stoichiometry, the study of the interactions of elements in ecological systems,  
47 is an organizing principle in ecology that provides a theoretical framework to explore how  
48 elements regulate plant growth, decomposition rates, and nutrient cycling at multiple scales  
49 (Elser et al. 2000). In soil, carbon-to-nitrogen (C:N) stoichiometry could be seen as a master  
50 variable that governs the flows of C and N between plants, microbes, and soils. Changes in soil  
51 C:N also reflect changes in soil C and N storage, which modify carbon cycle-climate feedbacks  
52 and nutrient limitation of plant growth, respectively. Further, soil C:N can be indicative of  
53 mechanistic changes in the system and represents the N requirement of C storage, important  
54 for land management aiming to increase soil C storage (Buchkowski et al. 2019, Cotrufo et al.  
55 2019). Indeed, as our understanding of soil organic matter (SOM) dynamics advances, the role  
56 of soil stoichiometry remains an important aspect of ecosystem biogeochemistry (Buchkowski et  
57 al. 2019). Despite this central role and advancing knowledge, the controls of SOM C:N

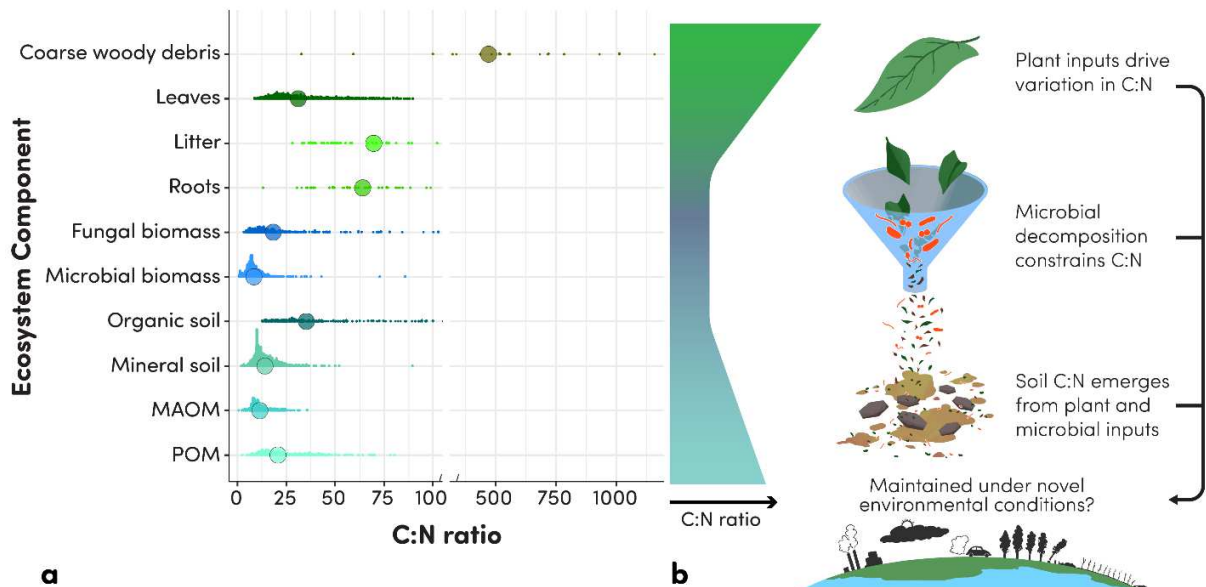
58 stoichiometry in process-based models of terrestrial biogeochemistry (“models” hereafter;  
59 Supplementary Table 1)—which both emerge from and are informed by measurements and  
60 theory (Blankinship et al. 2018)—have remained largely stagnant and mostly consist of the C:N  
61 ratios of plant and microbial inputs. However, numerous recent studies have identified additional  
62 plant, microbial, and physico-chemical controls of SOM C:N stoichiometry that are largely  
63 missing from model formulations (e.g., Cotrufo et al. 2019, Possinger et al. 2020, Song et al.  
64 2022; Amorim et al. 2022). These missing controls likely underlie global patterns in soil C:N and  
65 may be particularly important under global change scenarios where climate change, elevated  
66 CO<sub>2</sub>, and N enrichment (from fertilization or atmospheric deposition) may alter the availability of  
67 and demand for N (Terrer et al. 2016, Souza et al. 2021). The goal of this perspective is to  
68 evaluate controls of soil C:N with a focus on gaps in both our theoretical understanding and  
69 model formulations. We first describe the foundational representation of soil C:N controls  
70 currently present in most models. Then, we describe an emerging representation of soil C:N  
71 controls, derived from empirical work that is informing a more complete and nuanced theoretical  
72 understanding, with the ultimate goal of aligning this representation with formulations in models.  
73 Finally, we explore how implementing the emerging representation of soil C:N controls could  
74 influence predictions of soil C and N cycling under global change.

## 75 2. Foundational Representation of Soil C:N

### 76 2.1 *Conceptual understanding of soil carbon-to-nitrogen stoichiometry*

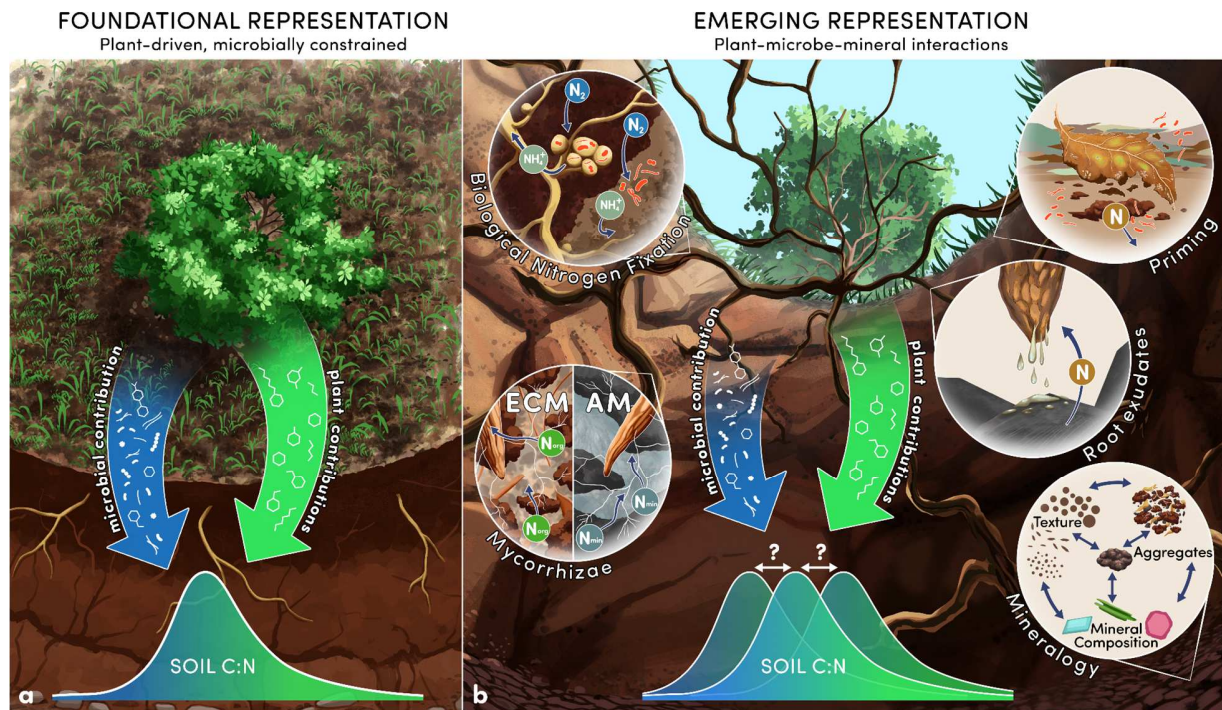
77 The influence of plant C:N on soil processes has been recognized for at least forty  
78 years, when lower C:N plant material was found to decompose more quickly than higher C:N  
79 plant material (Melillo et al. 1982, Enriquez et al. 1993). Faster decomposition of lower C:N plant  
80 material occurs, in part, because it is better aligned with the relatively lower and more strongly  
81 constrained C:N ratio of the microbes that decompose it (plant C:N = 9-1160; microbial biomass

82 C:N = 1.86; Figure 1; Cleveland and Liptzin, 2007). The relative stoichiometric homeostasis of  
83 the soil microbial biomass C:N thus drives soil C and N recycling, where microbes mineralize  
84 excess C or N not used to build their biomass to  $\text{CO}_2$  and ammonium, respectively. This  
85 process, termed consumer-driven nutrient recycling (Elser and Urabe, 1999), converts relatively  
86 high and variable plant C:N to relatively low and less variable C:N during microbial  
87 decomposition (Tipping et al. 2016). Indeed across multiple ecosystems and data sources we  
88 see a consistent decrease in the C:N stoichiometry of different ecosystem components as highly  
89 variable plant inputs pass through a more stoichiometrically constrained microbial filter to  
90 generate SOM (Figure 1). Previously, SOM was thought to largely consist of variably  
91 decomposed plant material, but it is now largely accepted that SOM also includes microbial  
92 materials that persist due to their physical or chemical inaccessibility to further decomposition  
93 (Cotrufo et al. 2013, Lehmann & Kleber, 2015, Kallenbach et al. 2016). Thus, the stoichiometry  
94 of bulk SOM reflects contributions of both higher C:N plant material and lower C:N microbial  
95 biomass and by-products. The stoichiometry of bulk SOM also depends on the relative  
96 contribution of different SOM fractions (Buchkowski et al. 2019). The relatively low C:N of stable  
97 SOM pools (e.g., mineral-associated organic matter or MAOM) results from the greater  
98 contribution of microbial material (von Lutzow et al. 2007), whereas the higher C:N of particulate  
99 organic matter (POM) is due to greater contributions of structural plant material (von Lutzow et  
100 al. 2007, Haddix et al. 2016; Figure 1a). This theoretical understanding informed a “foundational  
101 representation” of soil stoichiometry that guides conceptual models, where plant C:N drives  
102 SOM C:N variability and nutrient recycling, while microbial C:N constrains it. (Figure 2a).  
103 Additionally, environmental variables like temperature, moisture, and nutrient availability that  
104 control rates of microbial decomposition impact the balance between plant and microbial  
105 contributions to SOM C:N (Wieder et al. 2009), suggesting that changes to climate, nutrient  
106 pollution (e.g., N deposition), and environmental conditions may change the controls of soil C:N  
107 in the future.



109  
110  
111  
112  
113  
114  
115  
116  
117  
118  
119  
120  
121

**Figure 1.** (a) Empirically derived C:N ratios of different ecosystem components showing a narrowing of C:N ratios along the plant-microbe-soil continuum. Filled circles depict arithmetic means and small points arrayed as histograms depict individual observations. Data sources: coarse woody debris (Weedon et al., 2009); leaves (Dynarski et al., 2023); fresh litter and standing roots (NEON, 2023); fungal biomass (Zhang & Elser, 2017); microbial biomass (Xu et al., 2013); organic and mineral soil (Tipping et al., 2016); MAOM and POM (MAOM = mineral-associated organic matter; POM = particulate organic matter; Georgiou et al, 2022a). B) Conceptual depiction of the foundational representation of the decomposition process (funnel) that transforms relatively high plant C:N to relatively lower soil C:N, due to contribution of both plant and microbial materials to bulk SOM, with expected changes in the C:N ratio during this process. Earth with global change processes at bottom depicts uncertainty in the ability of the drivers above to simulate soil C:N under novel environmental conditions and thus the need to incorporate additional drivers of soil C:N beyond plant and microbe C:N.



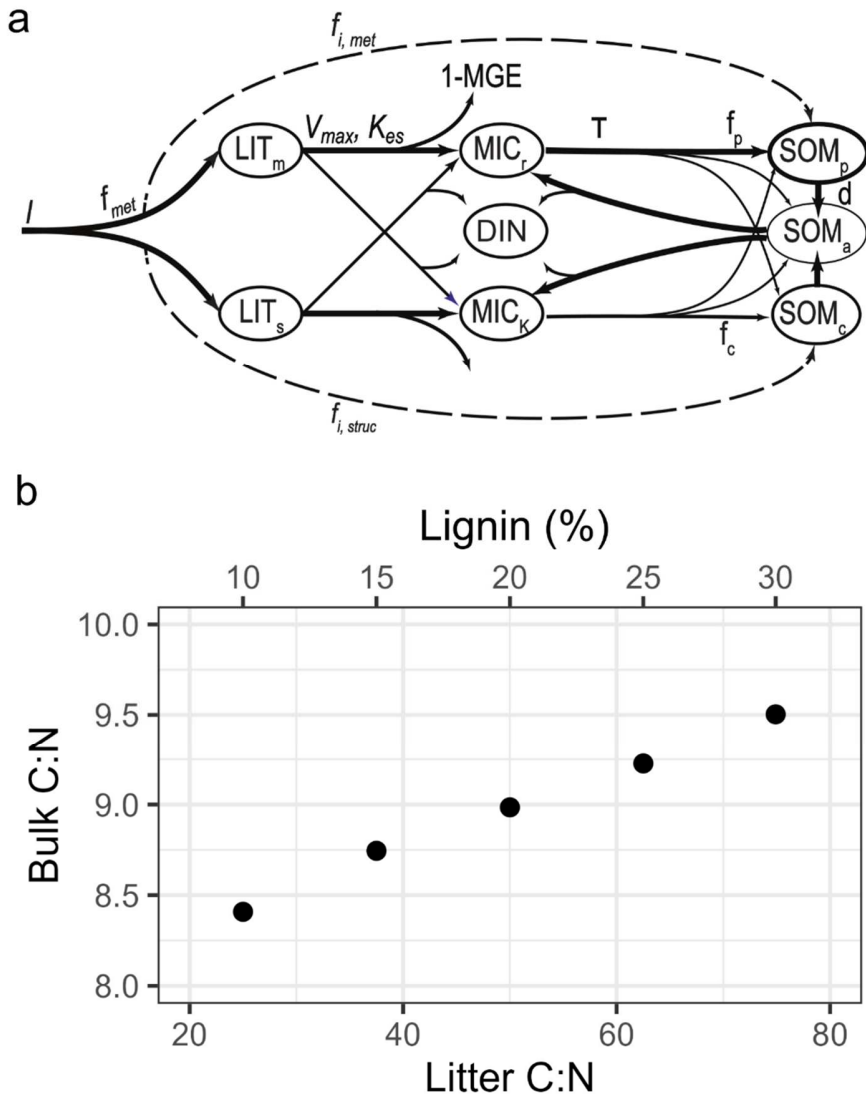
122  
123

124 **Figure 2.** Conceptual illustration showing foundational and emerging representations of the controls on  
125 C:N stoichiometry. (a) In the foundational representation, relatively high C:N plant material (green)  
126 combines with relatively low C:N microbial inputs (blue) to create the distribution of soil C:N values.  
127 Because plants have a wider range of C:N than microbes, plant C:N drives wider variation in soil C:N  
128 while microbial contributions constrain soil C:N, hence the right-skew of the histogram depicting soil C:N  
129 variation. In the foundational representation, this plant-centric focus is depicted as a "top-down" view of  
130 the soil C:N. (b) In the emerging representation, additional drivers of soil C:N that are typically absent  
131 from foundational representation of soil C:N are depicted (circular vignettes). Additional factors that may  
132 influence soil C:N can be broadly grouped into plant and microbe feedbacks and soil physico-chemical  
133 effects, and include the specific drivers of biological nitrogen fixation, mycorrhizae, priming, root  
134 exudates, and mineralogy (including soil texture, mineral composition, and aggregation). These drivers  
135 act through a diversity of mechanisms and thus can differentially influence C:N in ways that may be  
136 unrelated to initial plant C:N. This potential for variation in soil C:N due to the emerging drivers is depicted  
137 as shifts in the soil C:N histogram. In the emerging representation, this focus on processes occurring in  
138 the soil is depicted with a "bottom-up" view that emphasizes plant-microbe-mineral interactions.  
139

140 *2.2 Implementation of foundational representation in models*

141 Most current ecosystem biogeochemistry models (e.g. DayCent, PnET, or TEM) and  
142 land models that are used for global-scale projections (e.g. CLM, JSBACH, or LPJ-Guess;  
143 Davies-Barnard et al. 2020, Kou-Giesbrecht et al. 2023) are structured and parameterized with  
144 the foundational representation of soil C:N (Supplementary Table 1). Under these assumptions,  
145 simulated rates of soil C and N cycling reflect formulations of pool-specific turnover times, donor

146 and receiver pool stoichiometry, and C use efficiency (CUE, which determines the fraction of  
147 heterotrophic respiration; Parton et al. 1993, Parton et al. 1994, Thornton and Rosenbloom,  
148 2005). Nitrogen mineralization versus immobilization occurs to balance donor pool transfers of  
149 C and N with receiver pool stoichiometry. Generally, these models implicitly represent microbial  
150 activity (Schimel 2001), using environmentally sensitive first-order kinetics to define the turnover  
151 of litter and soil organic matter pools. The microbially-implicit modeling approach typically  
152 simulates down-regulation of decomposition rates when inorganic N availability is limiting, which  
153 generally occurs during transfers of material from high C:N litter to low C:N soil organic matter  
154 pools (Lee et al. 1992, Metherell et al. 1993, Parton et al. 1993, Bonan et al. 2013, Thomas et  
155 al. 2015). By contrast, models that explicitly represent microbial activity do not by default exhibit  
156 down-regulation of decomposition rates because of N limitation. For example, Kyker-Snowman  
157 et al. (2020) included overflow respiration of donor-pool C when N availability fails to meet the  
158 stoichiometric demands of decomposer biomass. This approach also eliminates the need to  
159 directly parameterize soil stoichiometry. Instead, soil C:N emerges from the relative contribution  
160 of microbial by-products (with a lower C:N ratio and narrower range) and plant detritus that  
161 bypasses the microbial filter and enters different SOM pools (Sulman et al. 2017, Zhang et al.  
162 2021, Eastman et al. 2023). This is exemplified in the microbially-explicit model MIMICS-CN,  
163 where soil C:N is strongly influenced by plant input chemistry and which we use in case studies  
164 throughout this paper (Figure 3). Despite differences in how soil C:N is determined in  
165 microbially-implicit vs -explicit approaches, both approaches rely on the foundational  
166 representation of soil C:N.



167

168

169 **Figure 3.** (a) Wiring diagram for MIMICS-CN model, which we use in case studies throughout this paper.  
170 Briefly, litter inputs ( $l$ ) are split into metabolic and structural pools ( $LIT_m$  and  $LIT_s$ ) which are decomposed  
171 by microbial communities having copiotrophic and oligotrophic growth strategies ( $MIC_r$  and  $MIC_k$ ,  
172 respectively), where both litter ( $f$ ) and microbial turnover ( $T$ ) can contribute to the physicochemically  
173 stabilized and chemically stabilized soil organic matter pools ( $SOM_p$  and  $SOM_c$ , respectively), and  $SOM_p$   
174 and  $SOM_c$  contribute to an available SOM pool ( $SOM_a$ ) that can be accessed by microbes. Detailed  
175 description of the model can be found in Kyker-Snowman et al. (2020) building upon Wieder et al. (2014).  
176 (b) MIMICS-CN simulations of bulk soil C:N in a hypothetical temperate deciduous forest where only the  
177 chemical quality (defined as the C:N ratio and lignin content) of litterfall inputs to surface soils are  
178 modified.

179

180

181 Model formulations that implement the foundational representation do represent  
182 dynamic flows of C and N during field decomposition, but falter in certain ecosystems (i.e.  
183 tundra and arid grasslands) and generally underestimate variation in soil C:N (Parton et al.  
184 2007, Bonan et al. 2013, Kyker-Snowman et al. 2020, Juice et al. in review). The accuracy and  
185 reliability of these models are insufficient for simulating the full spectrum of ecosystems and  
186 may falter under novel environmental conditions (e.g., global environmental change; Figure 1b,  
187 bottom; Wieder et al. 2019). For example, recent research shows that interactions between  
188 plants, microbes, and the soil matrix strongly regulate soil C and N cycling, and consequently  
189 SOM C:N stoichiometry (e.g., Keiluweit et al. 2015, Jilling et al. 2018, Possinger et al. 2020,  
190 Daly et al. 2021, Terrer et al. 2021). Representing these mechanisms is paramount for  
191 improving mechanistic representation of soil C:N and predicting changes in soil C:N under  
192 global change.

### 193 3. Emerging representation of soil C:N

194 The empirical evidence of important drivers beyond plant and microbe C:N that shape  
195 soil C:N ratios informs an “emerging representation” of the controls of soil C:N variation (Figure  
196 2b). We use the word “emerging” to explicitly acknowledge that many of the processes we  
197 describe below are already recognized as important for soil C:N in some subfields of soil  
198 science and represented in some models. However, we aim to clarify the importance of and  
199 collate these “emerging drivers” so that they can be aligned with model assumptions. We group  
200 these emerging drivers into plant and microbe feedbacks and soil physico-chemical effects that  
201 are absent from the foundational representation of soil C:N. The foundational representation  
202 considers plants and microbes as drivers of variability in soil C:N, and does not consider how  
203 soil C:N might feed back on the quantity and quality of plant inputs and subsequent microbial  
204 activity nor how minerals could act as a filter on soil C:N stoichiometry. Plant, microbial, and soil

205 physico-chemical drivers have the potential, at least in certain circumstances, to improve the  
206 mechanistic representations of modeled soil C:N, even if they do not alter predictions of spatial  
207 variation in soil C:N. We review the empirical evidence for the importance of these emerging  
208 drivers and whether they align with assumptions in models. We focus on drivers that are  
209 evidenced as empirically important because adding additional processes to models can require  
210 additional input data, parameter optimization, and computational costs. Thus, there must be  
211 careful consideration of the balance between model complexity and realism when adding  
212 additional processes to models. We note that no one model is likely able to represent all of the  
213 processes we discuss below, but that representing the emerging drivers in some models will  
214 allow for research questions better tailored to systems where a given driver is particularly  
215 important.

## 216 3.1 Plant and microbe feedbacks

### 217 3.1.1 Biological Nitrogen Fixation

218 Biological N fixation represents a process that could influence soil C:N in ways not  
219 captured in the foundational representation of soil C:N controls. N fixation occurs through two  
220 general pathways: as plant symbiotic N fixation, where N is fixed for direct plant use via a  
221 symbiotic relationship with root-nodulating bacteria, and as “free-living” N fixation, where N is  
222 fixed by both autotrophic and heterotrophic bacteria that occupy a diversity of non-vascular plant  
223 niches (e.g., soil, leaf litter, wood, etc.; Vitousek et al. 2013, Cleveland et al. 2022). Both forms  
224 contribute new N inputs that enhance relative plant and soil N content, and thus may be  
225 hypothesized to reduce soil C:N (Vitousek et al. 1987, Vitousek and Walker, 1989, Adams et al.  
226 2016, Gou et al. 2023). However, experimental and empirical studies have shown that invasion

227 and/or introduction of N-fixing plants can have positive, negative, or neutral effects on soil C:N  
228 (Johnson and Curtis, 2001, Liao et al. 2008).

229         Although N fixation has been implemented in many models, it is commonly simulated  
230 using phenomenological relationships between empirically derived N fixation rates and net  
231 primary production or evapotranspiration (Wieder et al. 2015, Meyerholt et al. 2016). Symbiotic  
232 N fixation (alone) is most often included in models as an addition of N to the plant pool. By  
233 contrast, when free-living N fixation is included in models, it is often represented as an addition  
234 of N to the mineral N pool (Metherell et al. 1993, Reed et al. 2011, Hartman et al. 2018,  
235 Lawrence et al. 2019). These formulations of N fixation could promote increased microbial  
236 activity and subsequent input to SOM pools when microbial growth is associated with increased  
237 labile plant material and reduced microbial N limitation, such as in CORPSE-FUN, thereby  
238 reducing SOM C:N (Sulman et al. 2017).

239         More mechanistic implementations of N fixation could more accurately simulate how N  
240 fixation shapes SOM C:N stoichiometry. Potential model improvements include representations  
241 of non-symbiotic, rather than solely symbiotic, N inputs, N fixation inputs based on both C  
242 supply and N demand (rather than one or the other), and benchmarking against new and  
243 emerging empirical estimates of global N fixation (Vitousek et al. 2013, Davies-Barnard and  
244 Friedlingstein, 2020). Improved model representations of N fixation would further advance  
245 models that simulate N fixation using a resource optimization strategy, which are currently the  
246 most advanced representations of N fixation (e.g., GFDL-LM3-BNF, CLM5, and CABLE; Fisher  
247 et al. 2010, Shi et al. 2016, Lawrence et al. 2019, Peng et al. 2020, Kou-Giesbrecht et al. 2021).  
248 Given that increasing atmospheric CO<sub>2</sub> concentrations are hypothesized to favor N fixation over  
249 much of the world (Novotny et al. 2007, Hungate et al. 2009, Nasto et al. 2019), improved  
250 representations of N fixation in models may be critical for accurately simulating soil C:N under  
251 global change.

252 3.1.2 Mycorrhizae

253 Mycorrhizal type and associated plant traits influence soil C:N stoichiometry and nutrient  
254 cycling through differences in their nutrient acquisition strategies. Ericoid- and ectomycorrhizal-  
255 (ECM) dominated ecosystems typically have higher litter and soil C:N ratios and slower rates of  
256 nutrient cycling compared to arbuscular mycorrhizal- (AM) dominated ecosystems (Phillips et al.  
257 2013, Averill et al. 2014). The direct connections between plant litter quality and soil  
258 stoichiometry are captured by the plant-to-soil pathway in the foundational representation of soil  
259 C:N. However, mycorrhizae allow for a two-way relationship between plants and soil. As  
260 mycorrhizae receive C from plant roots, they can either produce enzymes to mine nutrients from  
261 SOM (ECM) or expand their hyphal network to more efficiently exploit soil inorganic N (AM;  
262 Brzostek et al. 2013, Midgley et al. 2016, Tedersoo and Bahram, 2019). Strategies related to  
263 these different nutrient economies may be particularly important for biogeochemistry in forest  
264 ecosystems, which can vary in the relative abundance of mycorrhizal types, and in ecosystems  
265 experiencing shifts in plant species composition, such as shrub encroachment in the Arctic  
266 (Wookey et al. 2009). Yet, explicit representations of these plant-mycorrhizal relationships are  
267 largely missing from models.

268 Some attempts have been made to represent plant-mycorrhizal relationships in models  
269 with variations in belowground plant C inputs across mycorrhizal type and soil N availability  
270 (Baskaran et al. 2017, Sulman et al. 2017, He et al. 2018, Shi et al. 2019, Huang et al. 2022).  
271 Overall, these modeling experiments show that incorporating mycorrhizae increases model-  
272 observation agreement of soil C stocks and C:N ratios. Meanwhile, they suggest that simulating  
273 plant-mycorrhizal relationships may constrain the impacts of climate change on soil  
274 biogeochemistry and plant productivity. For example, as nutrient demand increases with  
275 elevated CO<sub>2</sub>, ECM associations allow plants to mine SOM for N, enhancing plant productivity  
276 to a greater extent than AM systems that are less likely to mine N from SOM (Terrer et al.

277 2021). At the same time, this process typical of ECM-dominated ecosystems can increase  
278 competition between ECM and free-living saprotrophs, reducing the overall decomposition of  
279 SOM by saprotrophs and increasing soil C stocks and C:N ratios (Averill et al. 2014). Thus,  
280 incorporating these plant-mycorrhizal associations into models may also capture the divergent  
281 responses of forest ecosystems with different mycorrhizal associations to global changes like  
282 elevated CO<sub>2</sub> (Sulman et al. 2019), as has been observed at Free-Air Carbon Enrichment  
283 (FACE) sites (Terrer et al. 2016).

284

### 285 3.1.3 Plant priming of soil microbial activity

286 Soil priming, the accelerated decomposition of SOM via inputs of plant C, is a process  
287 with complex mechanistic underpinnings and highly variable responses to global changes  
288 (reviewed in Bernard et al. 2022). In some cases, plant priming may align with the foundational  
289 understanding of the plant-soil-stoichiometric continuum, where greater decomposition of fresh  
290 plant input increases microbial contributions to SOM and lowers soil C:N (Chen et al. 2014).  
291 However, at least three mechanisms may drive soil responses that likely differ from what is  
292 captured using foundational representations of soil C:N. First, higher soil microbial activity under  
293 priming may simultaneously accelerate decomposition rates of C-rich POM (in addition to  
294 decomposition of fresh plant input), reducing bulk C stocks and decreasing soil C:N (Bernard et  
295 al. 2022). Second, in nutrient-limited conditions, selective mining of N from SOM can occur  
296 when soil microbes use labile plant exudates as an energy source and preferentially immobilize  
297 N or N-rich material from SOM, thereby increasing SOM C:N (Chen et al. 2014, Hicks et al.  
298 2020, Na et al. 2022). Third, priming could alter microbial community composition, favoring  
299 microbial functional groups that preferentially degrade substrates with high or low C:N ratios  
300 (Geyer et al. 2020). Therefore, representation of priming may be particularly important in  
301 scenarios where we expect changes to plant input quantity and quality (e.g., changes in plant

302 community composition or allocation) and nutrient limitation (e.g., elevated CO<sub>2</sub>, Mason et al.  
303 2022).

304 Priming effects are not typically included in first order models because SOM turnover  
305 times are only modified by environmental scalars (e.g., temperature and moisture). A notable  
306 exception is the ORCHIDEE-PRIM model, which represents priming by modifying turnover times  
307 with changes in plant productivity, but only represents C (Guenet et al. 2016). Explicit  
308 representation of microbial activity, however, may provide more sophisticated, testable  
309 representations of priming mechanisms, including higher turnover rates, microbial N-mining, or  
310 preferential degradation of different SOM pools by different microbial functional types (Schimel,  
311 2023). Indeed, microbially explicit models may include an emergent representation of priming  
312 due to relationships between substrate availability and microbial growth (Schimel, 2023).  
313 Current models that specifically simulate priming operate on relatively short or small temporal or  
314 spatial scales, with the goal of better understanding the complex interactions of microbes, OM,  
315 and minerals and dynamics of priming (Bernard et al. 2022). For example, the SYMPHONY  
316 model (Perveen et al. 2014) simulates N-mining in priming, but only at landscape to ecosystem  
317 scales. However, the importance of incorporating priming at larger scales is increasingly  
318 recognized (Terrer et al. 2021).

### 319 3.1.4 Root exudation of organic acids

320 In addition to root exudates that accelerate microbial activity and N mineralization via  
321 priming, plants also produce exudates that can directly increase SOM availability. Root  
322 exudation of organic acids (e.g., oxalic acid) can directly destabilize MAOM by locally lowering  
323 the pH in the rhizosphere, thereby chelating or competing with previously mineral-bound organic  
324 matter (Keiluweit et al. 2015, Jillion et al. 2018). This effectively promotes faster turnover of  
325 organic matter, as MAOM typically has long turnover times and low C:N ratios (Lavallee et al.  
326 2020). Thus, organic acids may increase the availability of decomposable substrates and

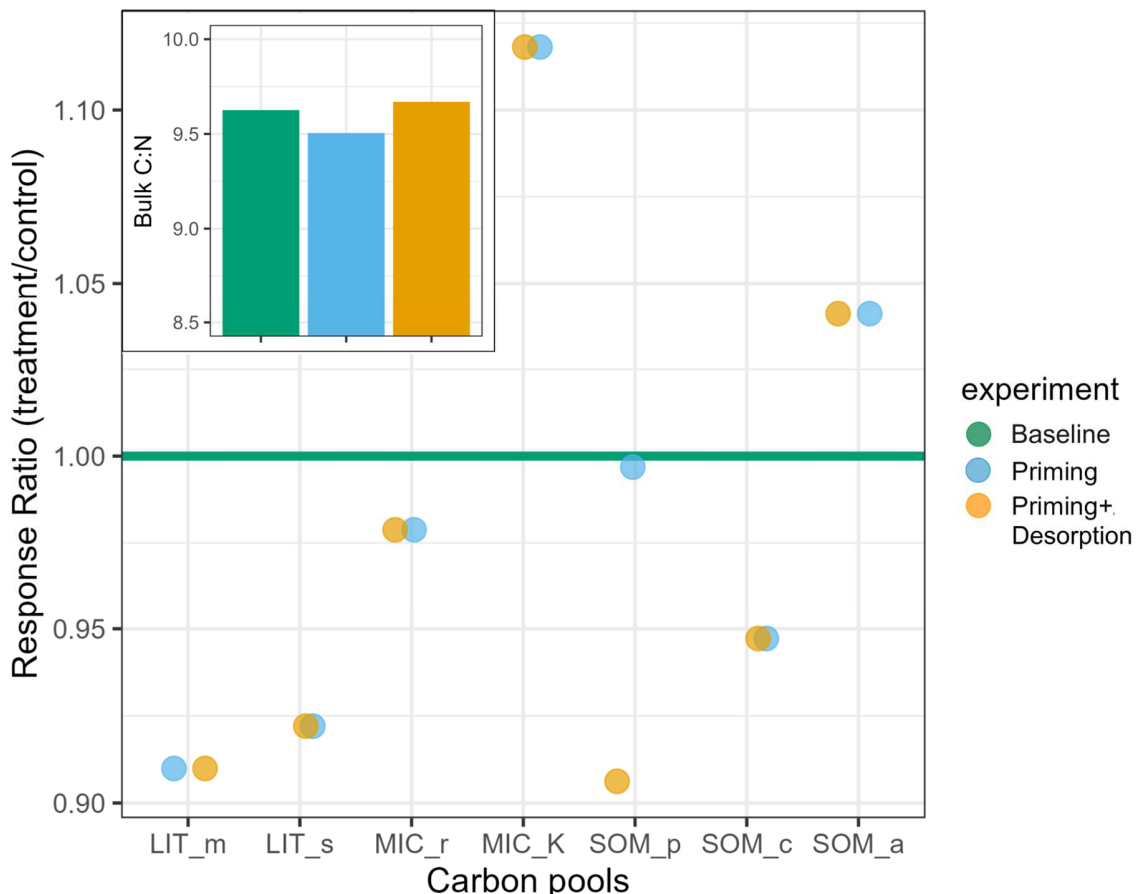
327 accelerate rates of N mineralization and plant N uptake (Jilling et al. 2018, Daly et al. 2021).

328 Given the relatively low C:N of MAOM, its decomposition would tend to drive a loss of N-rich  
329 OM and subsequently increase the bulk soil C:N ratio.

330 Currently, depolymerization of SOM by enzymes and decomposers is considered the  
331 rate limiting step for N mineralization (Schimel and Bennet, 2004, Mooshammer et al. 2014),  
332 which ultimately constrains plant N availability and primary production in models. MAOM is often  
333 considered inaccessible to plants and microbes, though recent advances suggest that it may be  
334 an important plant N source (Jilling et al. 2018, Lavallee et al. 2020, Daly et al. 2021). As such,  
335 the direct effects of plant root inputs on the turnover of MAOM is virtually absent in models.  
336 Instead, in most models MAOM-like pools are represented with long turnover times that are  
337 modified by environmental scalars (temperature or moisture) and potentially modified by soil  
338 properties like soil texture or clay content. Very few models actually represent root exudation,  
339 and those that do only partially represent complex priming effects. For example, FUN-CORPSE  
340 only considers mycorrhizal response to exudates (Sulman et al. 2017). The closest  
341 approximation may be from the model ecosys, which simulates root exudation and exchange of  
342 organic C for organic N and P (Grant et al. 2016, Mekonnen et al. 2019, Chang et al. 2020,  
343 Bouskill et al. 2022). However, none of these models represent direct destabilization of MAOM  
344 caused by root exudation of organic acids. Indeed, consideration of mycorrhizae, priming, and  
345 organic acids introduces additional complexities to the emerging representation of soil C:N that  
346 are worth exploring further in models. As a preliminary step towards this exploration, we  
347 investigate the influence of priming, which could both increase or decrease soil C:N, and that of  
348 root exudation of organic acids, which we expect to increase soil C:N, below.

349 3.1.5 Biotic Case Study: Simulating priming and desorption in the MIMICS-  
350 CN model

351 As a case study, we explored the potential effects of root exudation that causes priming  
352 and desorption (via exudation of organic acids) on steady state pools simulated by the MIMICS-  
353 CN model (Kyker-Snowman et al. 2020, Eastman et al. 2023). We use this case study and  
354 those in following sections (sections 3.2.2 and 4.1) to illustrate the potential importance of the  
355 emerging drivers of soil C:N but acknowledge that studies at larger scales and with different  
356 models will be needed to fully evaluate the importance of the emerging drivers for soil C:N. All  
357 experiments were performed in a hypothetical temperate deciduous forest with identical climate,  
358 litterfall inputs, litter quality and soil conditions. In all simulations, we calculated bulk soil C:N  
359 ratios as well as steady state C pools to explore the mechanisms driving changes in bulk soil  
360 C:N. The baseline simulation received root exudates as inputs to the metabolic litter pool ( $LIT_m$ )  
361 with a defined C:N ratio of 15 (Kyker-Snowman et al., 2020). This baseline experiment was  
362 designed to illustrate an implicit representation of root exudation fluxes, which are handled with  
363 the same stoichiometry as relatively labile plant detritus. At steady state, the baseline  
364 experiment simulated a bulk soil C:N ratio of 9.6, total steady state C of  $6.4 \text{ kgC m}^{-2}$ , microbial  
365 biomass was 1.5% of soil C pools, and 43% of SOM was in the  $SOM_p$  pool (physico-chemically  
366 protected SOM, which we equate with MAOM; Figure 4). The bulk soil C:N stoichiometry and  
367 fraction of the  $SOM_p$  pool were lower than median observational estimates (Figure 5, discussed  
368 below), which is consistent with previous work with MIMICS-CN (Kyker-Snowman et al. 2020).  
369



370  
371  
372  
373  
374  
375  
376

**Figure 4.** Response ratio of C stocks in various pools of MIMICS-CN under priming (blue) and priming+desorption (yellow) experiments as compared to the baseline (green). Bulk soil C:N ratios for each experiment are shown in the inset plot. LIT\_m = metabolic litter; LIT\_s = structural litter; MIC\_r = copiotroph microbial biomass; MIC\_K = oligotroph microbial biomass; SOM\_p = physically protected SOM; SOM\_c = chemically protected SOM; SOM\_a = active SOM.

377  
378  
379  
380  
381  
382  
383  
384

In a second “priming” experiment we more explicitly considered the effects of priming via root exudation by transferring 10% of metabolic litter inputs to the microbially-available SOM pool (SOM<sub>a</sub>) at initialization. This simulation was designed to represent potential plant priming of soil microbes without changing the quantity or chemical quality of plant inputs to soils. This representation of priming increased total microbial biomass and the relative abundance of oligotrophic microbes (MIC<sub>K</sub>), which resulted in a slightly higher microbial biomass C:N compared to the baseline experiment (7.0 vs. 6.9, respectively). In response to priming, microbial community shifts accelerated decomposition of litter and SOM<sub>c</sub> pools, relative to the

385 baseline simulation, which slightly decreased total C stocks and bulk soil C:N ratio (6.2 kgC m<sup>-2</sup>  
386 and 9.5, respectively; Figure 4). Broadly, these results are consistent with stimulation of  
387 oligotrophic microbial communities that have a competitive advantage over copiotrophic  
388 communities when utilizing more chemically complex substrates (Fontaine et al. 2003). In our  
389 simulations, oligotrophs increased in relative abundance and produced more enzymes that  
390 decompose litter and SOM<sub>C</sub> (comparable to POM). Yet, the magnitude of the effects on steady  
391 state pools and bulk soil stoichiometry were relatively small. The subtle changes in soil C stocks  
392 and C:N ratio may indicate that either the priming effect does not exert a strong control of  
393 steady-state behavior in the model, or that our simple priming experiment does not capture  
394 more complex priming mechanisms (Hicks et al. 2020, Karhu et al. 2022, Na et al. 2022).  
395 However, this simple priming experiment captures priming-induced directional changes in  
396 microbial community composition and soil C:N that are consistent with theoretical expectations,  
397 suggesting that more work is needed to evaluate whether the magnitude of these changes are  
398 appropriate.

399 In a third “priming+desorption” experiment, we considered the potential role of organic  
400 root acids liberating MAOM. Here, we repeated the priming experiment, but also increased the  
401 desorption rate of SOM<sub>P</sub> (comparable to MAOM) by 10% relative to the baseline simulation.  
402 Increasing the desorption rate decreased the size of the SOM<sub>P</sub> pool relative to both the baseline  
403 and priming experiments. As the SOM<sub>P</sub> pool in MIMICS has a relatively low C:N ratio, reducing  
404 the size of this soil fraction increases bulk soil C:N ratios slightly above baseline values (9.7;  
405 Figure 4). Again, the changes in total soil C stocks and C:N stoichiometry associated with this  
406 simplistic consideration of organic acids liberating MAOM are relatively small, but the direction  
407 of these changes are in line with theoretical expectations (Keiluweit et al. 2015, Jilling et al.  
408 2018). This experiment also underscores the data and knowledge gaps associated with the  
409 extent to which organic acids from root exudates may accelerate desorption of MAOM (Jilling et  
410 al. 2021). It is technically challenging to quantify these fluxes even in lab incubations with

411 artificial roots at sub-millimeter scales (Keiluweit et al. 2015) and scaling these insights to larger,  
412 more field-relevant scales remains speculative. Progress likely requires a more advanced  
413 empirical understanding and representation of soil physico-chemical properties and their  
414 influences of SOM dynamics.

## 415 3.2 Soil physico-chemical effects

### 416 3.2.1 Mineralogy

417 Three interrelated factors provide a robust 'bottom-up', soil-driven regulation of soil C:N  
418 ratio: soil texture, mineral composition, and aggregation. Texture, which describes the relative  
419 proportions of sand, silt, and clay particles, is known to impact the C:N stoichiometry of SOM  
420 because charged clay surface particles can form stable associations with charged moieties like  
421 amino groups (Jilling et al. 2018), leading to N enrichment in clay fractions compared to sand  
422 fractions (Haddix et al. 2016, Amorim et al. 2022). Increased clay content increases total  
423 surface charge and surface area available for organo-mineral interactions that form MAOM.  
424 MAOM is often defined as the size fraction associated with silt and clay (Leuthold et al. 2022).  
425 Thus, as this fraction increases, we expect more organic matter to accumulate in MAOM with  
426 comparatively low C:N ratio. However, silt may contain primary particles, have substantially less  
427 surface charge, and be a microsite for accumulating fungal residues with relatively high C:N  
428 ratios (Six et al. 2006, von Lutzow et al. 2007). These factors can lead to variation in the  
429 relationship between MAOM fractions and soil C:N ratios that depend upon the relative  
430 proportions of silt and clay and at the same time their geochemical properties.

431 Some studies indicate that N-rich organic compounds may be preferentially adsorbed by  
432 certain types of soil colloids (Kaiser and Zech, 2000, Kleber et al. 2005, Mikutta et al. 2010, Yu  
433 et al. 2013, Jilling et al. 2018, Zhao et al. 2020), potentially accounting for variable C:N ratios

434 depending on mineral composition. Recent studies show sorption of both N-rich microbial  
435 products and N-free aromatic compounds to soil mineral surfaces (Kramer et al. 2017, Kopittke  
436 et al. 2018, Gao et al. 2021). This variation in sorption may arise from variation in surface  
437 charge or nano-scale topographic characteristics of minerals (Vogel et al. 2014). Iron (Fe) and  
438 aluminum (Al) may be uniquely strong binding agents in soils rich in these minerals (e.g.,  
439 Andisols). These soils exhibit preferential binding of low C:N SOM in organo-metal  
440 nanocomposites (<2  $\mu$ m) and associations between N-rich compounds and ferrihydrite (an Fe  
441 mineral) concentrations (Asano et al. 2018, Zhao et al. 2020). Importantly, Fe content has been  
442 shown to be negatively associated or uncorrelated with clay content in certain environments,  
443 indicating the unique influence of Fe minerals (Rasmussen et al. 2018, Zhao et al. 2020). Soil  
444 pH can also interact with mineral composition, through controlling the relative importance of  
445 select SOM stabilization mechanisms (e.g., organo-metal complexation in acidic soils to  
446 exchangeable calcium in basic soils; Rasmussen et al. 2018). For example, the amount of  
447 pedogenic oxide-hydroxides affects the density of hydroxyl-groups and the formation of mineral  
448 associations via ligand exchange; pH can affect the protonation of these hydroxyl-groups and  
449 thereby the propensity for ligand exchange (Kleber et al. 2015). Thus, pH interacts with mineral  
450 type to drive relative sorption of C or N, potentially driving N-enrichment in Fe and Al minerals in  
451 humid and acidic environments and in phyllosilicates in dry and basic environments.

452 The texture and mineral composition of soil also regulate soil aggregation, which is  
453 another control over soil C:N ratios (Schweizer et al. 2023). Aggregates are clusters of soil  
454 particles (sand, silt, clay) held together by various organic and inorganic binding agents.  
455 Aggregation processes influence the types of organic matter stabilized and the corresponding  
456 C:N ratios vary based on the aggregate size, formation, and binding mechanisms, all of which  
457 depend on numerous factors, including mineral and organic C content, faunal activity, and land  
458 cover (Elliott 1986, Fonte et al. 2007, An et al. 2010, Maaß et al. 2015, Haddix et al. 2020). For  
459 instance, it is known that microaggregates (< 250  $\mu$ m) accumulate N-rich compounds, primarily

460 derived from microbial sources, and efficiently form MAOM (Fulton-Smith and Cotrufo, 2019). In  
461 contrast, larger macroaggregates ( $> 250 \mu\text{m}$ ) typically form around POM with high C:N ratios  
462 (Six et al. 2000). Roots and certain fungal hyphae also stabilize macroaggregates, and in the  
463 process their biomass becomes somewhat protected from decomposition within the aggregate  
464 (Graf and Frei, 2013, Lehmann et al. 2020). Tillage and other destabilizing forces that break  
465 apart larger aggregates speed up the decomposition of POM. This favors the accumulation of  
466 smaller, more resistant, and stable aggregates filled with lower C:N ratio SOM, ultimately  
467 resulting in lower bulk soil C:N (Grandy and Robertson, 2007).

468 In most soil biogeochemical models, minerals can indirectly control bulk soil  
469 stoichiometry by modulating the proportion and persistence of organic matter in mineral-  
470 associated pools. Given the ubiquity of measurements, most models use soil texture as a proxy  
471 for mineral sorptive capacity (Rasmussen et al. 2018, Sulman et al. 2018, Georgiou et al. 2021).  
472 In particular, some models use clay content (e.g., MIMICS and CORPSE; Wieder et al. 2019a),  
473 while many others use the sum of clay and silt content (e.g., Millennial, COMISSION, MEMS;  
474 Abramoff et al. 2018, Aherns et al. 2020, Zhang et al. 2021). Mineral-associated OM pools in  
475 most models are primarily composed of microbial byproducts and necromass with relatively low  
476 C:N ratios, and to a lesser degree from direct sorption of dissolved or particulate organic matter;  
477 thus, texture ultimately acts as a control of bulk soil C:N stoichiometry. Only a subset of models  
478 currently represent mineral composition effects via equations relating pH and MAOM – namely,  
479 the Millennial, ecosys, and MEMS models (Grant et al. 2012, Zhang et al. 2021, Abramoff et al.  
480 2022, this issue). The Millennial and COMISSION models also include broad classes of  
481 mineralogy by separating soils into low- and high-activity minerals, based on whether soils are  
482 dominated by 1:1 or 2:1 clays, respectively (Aherns et al. 2020, Abramoff et al. 2022, this issue).  
483 Aggregation is a possible pathway for mineral control over soil C:N that only two C-only models  
484 have incorporated. Both AggModel and Millennial allow for both POM and MAOM to be  
485 captured in aggregates, whereas AggModel represents the hierarchy of micro- and macro-

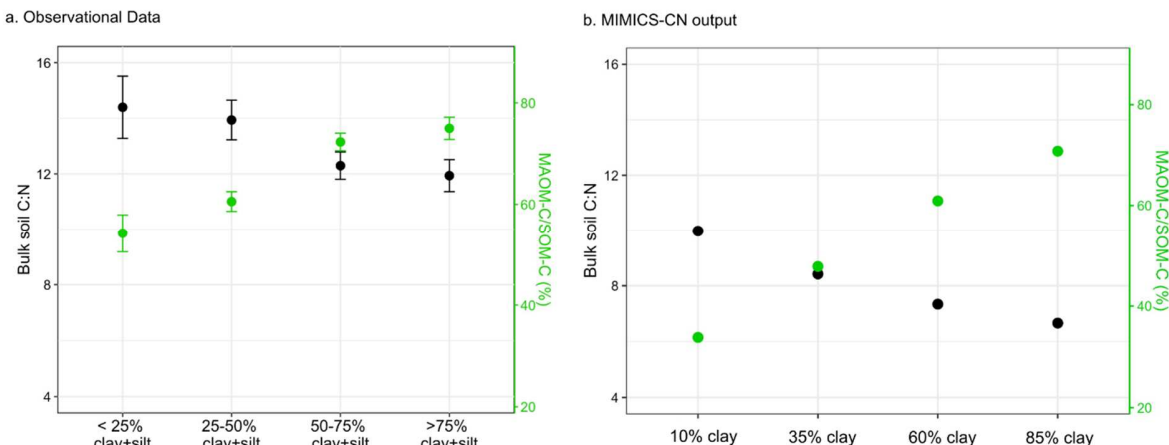
486 aggregates and Millennial has a single aggregate pool (Segoli et al. 2013, Abramoff et al. 2018).  
487 While neither AggModel nor Millennial currently considers N, protection of POM in aggregates  
488 might allow for higher C:N POM pools to persist, effectively increasing soil C:N. The frameworks  
489 developed in these models could someday help to understand the relationship between soil C:N  
490 and aggregate formation. To gain a preliminary understanding of the role of mineralogy in  
491 shaping soil C:N ratios we evaluate the relationships between SOM fractions, mineral variables,  
492 and soil C:N in both empirical data and models.

493 3.2.2 Physico-chemical Case study: Evidence for proxy variable inclusion in  
494 models

495 For almost 30 years, soil scientists have called for correspondence between measured  
496 and modeled pools of SOM (Christensen et al. 1996, Elliot et al. 1996, Blankenship et al. 2018)  
497 and, increasingly, models are formulated to model measurable pools of SOM from physical  
498 fractionations (Luo et al., 2014; Abramoff et al. 2018, Robertson et al. 2019). MAOM,  
499 operationally defined as the pool associated with silt and clay, is expected to preferentially  
500 contain microbial residues and consequently have a relatively low C:N ratio (Grandy et al. 2007,  
501 Lavallee et al. 2020), presumably leading to positive associations between silt+clay content and  
502 MAOM content, and negative associations of each of these with soil C:N. However, the strength  
503 of silt and clay control of stabilization of organic matter and, consequently, soil C:N, especially  
504 as compared to other mineralogical factors, remains contentious in theoretical and empirical  
505 work and variable in model formulations (Bailey et al. 2017; Rasmussen et al. 2018, Sulman et  
506 al. 2018, Wieder et al. 2018).

507 We explored the potential strength of silt and clay control, as well as several proxy  
508 variables as emerging indicators of mineral effects on C:N stoichiometry in models and in  
509 observational synthesis data, namely Georgiou et al. (2022a, b) and the Soils Data

510 Harmonization database (SoDaH; Wieder et al. 2021). Using Georgiou et al. (2022a), we found  
 511 soil C:N was lower in soils with higher proportions of silt+clay (Figure 5a). These silt+clay-rich  
 512 soils were also associated with a greater proportion of C in MAOM (Figure 5a), consistent with  
 513 theoretical understanding of MAOM (Lavallee et al. 2020). This observation is already captured  
 514 in MIMICS-CN (Figure 5b) and could likely be demonstrated with other models that use SOM  
 515 pool structures that represent MAOM and POM (e.g., MEMS, Millennial, and CORPSE; Sulman  
 516 et al. 2017, Zhang et al. 2021, Abramoff et al. 2022, this issue). These findings support calls for  
 517 further work benchmarking modeled SOM pools to measured ones (Berardi et al. 2020).  
 518 Currently, this benchmarking has only been carried out for a few models with and without these  
 519 measurable pools explicitly represented (Zimmerman et al. 2007, Zhang et al. 2021). Given  
 520 strong relationships between SOM pools and soil C:N, greater benchmarking efforts are likely to  
 521 improve confidence in simulations of soil C:N as well as soil biogeochemistry more broadly.



522  
 523 **Figure 5.** Bulk soil stoichiometry (C:N ratio; left y-axis, black points) and percentage of bulk soil organic  
 524 carbon that is mineral-associated (right y-axis; green points) across different soil texture regimes. (a) Soil  
 525 texture regimes are summarized by ranges in clay plus silt percentages. Points and error bars represent  
 526 means  $\pm$  95% confidence intervals on the mean from an observational synthesis of soil fractions  
 527 consisting of > 1200 measurements (n = 166, 388, 411, and 261 in the < 25%, 25-50%, 50-75%, >75%  
 528 clay + silt content regimes, respectively). (b) MIMICS-CN output for a hypothetical temperate deciduous  
 529 forest for soils with different amounts of clay, which is the controlling variable for sorption in MIMICS-CN,  
 530 rather than silt+clay. MAOM-C/SOM-C is calculated from MIMICS output as  
 531 SOMp/(SOMa+SOMc+SOMp)\*100%.

532

533            While our data suggest that bulk soil C:N is partly controlled by soil texture, the utility of  
534 other proxies for mineralogy is underexplored. To investigate the relevance of other  
535 mineralogical factors, we compared drivers of soil C:N in the SoDaH database to those in model  
536 simulations. For the observational data, we filtered the SoDaH database to isolate topsoil (< 20  
537 cm) data from studies that measured soil C:N and litter C:N. We generated model data by  
538 running global simulations of a microbially-explicit (MIMICS-CN; Kyker-Snowman et al. 2020)  
539 and a microbially-implicit (CASA-CNP; Wang et al. 2010) model forced with the same globally-  
540 gridded forcing data in a biogeochemical testbed (Wieder et al. 2018; detailed in Supplementary  
541 Material A). We then used multiple linear regressions (MLRs) to determine which variables  
542 emerged as important relative drivers of measured (SoDaH) and modeled (MIMICS-CN and  
543 CASA-CNP) soil C:N (detailed in Supplementary Material A). We analyze these below as  
544 qualitative comparisons, given the different geographic extents and data coverage between the  
545 observational data and models. For both measured and modeled data, we considered a three-  
546 factor MLR with mean annual temperature (MAT), clay content, and litter C:N as predictors for  
547 measured or modeled soil C:N. We also considered a seven-factor MLR with additional  
548 mineralogical factors as predictors for measured soil C:N, to evaluate which of these may be  
549 missing from model formulations (Table 1). For the three-factor MLRs, MIMICS-CN reasonably  
550 captured the relative importance of drivers in the SoDaH database whereas CASA-CNP  
551 depicted lower relative importance of clay, likely because it uses clay+silt to compute passive C  
552 formation, and higher relative importance of litter C:N, aligning with the more foundational  
553 representation of soil C:N (Table 1). Notably, the CASA-CNP MLR likely had a very low  $R^2$  value  
554 because it has prescribed ranges for the C:N of various pools and bulk C:N stems from the  
555 balance across those pools, exemplifying how fixed pool C:N fails to capture important drivers of  
556 soil C:N. In contrast with the three-factor MLRs, the seven-factor MLR with all possible proxies  
557 identifies clay, Fe, Al, and pH as the strongest relative drivers of measured soil C:N (Table 1).  
558 This suggests mineral composition, with Fe, Al, and pH as proxies, in addition to soil texture

559 (e.g., clay), are important drivers of soil C:N relative to the variables considered here. However,  
 560 mineral composition control of organic matter stabilization, and consequently soil C:N, is  
 561 represented in few models (Aherns et al. 2020, Abramoff et al. 2022, this issue).

562 **Table 1.** Results from multiple linear regression (MLR) analyses of a subset of the SoDaH database and  
 563 model outputs (Supplementary Material A). The dependent variable in each model is observed or  
 564 modeled soil C:N. Relative importance percentages show the percentage of the total variance explained  
 565 by each statistical model that a given individual variable explains. “NA” indicates a variable that was not  
 566 included in a given model. Greener cells have higher relative importance percentages. MAT is mean  
 567 annual temperature; MAP is mean annual precipitation; Fe<sub>ox</sub>, Al<sub>ox</sub>, and Si<sub>ox</sub>, and Fe<sub>dith</sub>, Al<sub>dith</sub>,  
 568 and Si<sub>dith</sub>, are oxalate-extractable and dithionite-extractable iron, aluminum and silica, respectively.

		Relative importance percentage																	
MLR type	n	R <sup>2</sup>	AIC	Litter										Fe <sub>ox</sub>	Al <sub>ox</sub>	Si <sub>ox</sub>	Fe <sub>dith</sub>	Al <sub>dith</sub>	Si <sub>dith</sub>
				MAT	Clay	C:N	MAP	Depth	pH	Fe <sub>ox</sub>	Al <sub>ox</sub>	NA	NA						
SoDaH observations	239	0.28	607	20.9%	46.5%	32.6%	NA	NA	NA	NA	NA	NA	NA	NA	NA	NA	NA	NA	
SoDaH observations	239	0.52	386	9.7%	15.5%	9.4%	8.7%	1.9%	10.5%	4.5%	9.3%	4.9%	11.1%	12.5%	1.8%				
MIMICS-CN model	2697	0.80	3318	31.1%	31.4%	37.5%	NA	NA	NA	NA	NA	NA	NA	NA	NA	NA	NA	NA	
CASA-CNP model	2697	0.06	7500	32.7%	2.8%	64.6%	NA	NA	NA	NA	NA	NA	NA	NA	NA	NA	NA	NA	

569  
 570 The concept of a “mineral filter” (Mikutta et al. 2019) acting as a bottom-up control of  
 571 SOM composition is supported overall by our analyses (i.e. the high relative importance of silt  
 572 and clay, pH and specific extractable metals; Figure 5; Table 1). Although the patterns observed  
 573 here do not definitively justify incorporating new mineral-related variables or processes into  
 574 models, they could be explored further in models or in field or lab experiments. Field  
 575 experiments could be used to explore possible mechanistic relationships between pH and  
 576 mineral composition. Using such a relationship, pH is an easily measured variable that could be  
 577 used to improve models, for example by making the model coefficient of clay stabilization  
 578 dependent on pH, as in the MEMS (Zhang et al. 2021) and Millennial (Abramoff et al. 2022, this  
 579 issue) models. The relative importance of dithionite-extractable Fe and Al in driving soil C:N in  
 580 our results also supports the importance of mineral composition. Increased use of chemical

581 extractions, which are more expensive and less widely measured, may be useful in identifying  
582 the specific minerals (e.g. Fe and Al oxides) that stabilize low C:N microbial residues  
583 (Rasmussen et al. 2018). More widespread measurements of specific soil mineralogy coupled  
584 to detailed mechanistic studies exploring the affinities of different minerals for N-enriched  
585 organic moieties (e.g. amino acids) may provide clarity about the role of edaphic factors in  
586 filtering SOM and soil C:N. These measurements would allow proxies like pH and soil Fe and Al  
587 oxides to be included in models as external parameters, used during model initialization, or  
588 even dynamic state variables, as has been done for redox reactions (Maggi et al. 2008; Rizzo et  
589 al. 2014; Calabrese & Porporato, 2019). Representing dynamic pH or mineralogy could be  
590 particularly important under variable soil moisture, N or heavy metal pollution, or when  
591 considering how pedogenic processes influence organic matter stabilization at millennial  
592 timescales. Better representation of mineralogy, as well as the plant and microbial drivers  
593 above, will be key for models' ability to predict soil C:N under global change.

## 594 4. Implications for Studying Global Change

595 Global changes, such as rising atmospheric CO<sub>2</sub>, N deposition, and changing climate  
596 influence the entire plant-soil system. For example, elevated CO<sub>2</sub> generally increases and N  
597 deposition generally decreases the C:N of vegetative tissues and litter entering the soil system  
598 (Yang et al. 2011, Sardans et al. 2012, Yue et al. 2017, Sun et al. 2020). While these changes  
599 to vegetation C:N stoichiometry will likely introduce numerous feedbacks in the plant-soil  
600 system, the net effects of these opposing influences are not well characterized. Models are  
601 valuable tools for exploring the trajectories of these global changes and understanding the  
602 possible large-scale implications of variable controls of soil stoichiometry for C and N dynamics  
603 (Wieder et al. 2019b). Examining elevated CO<sub>2</sub> and N deposition in coupled C-N models  
604 therefore presents a good opportunity to evaluate our foundational versus emerging

605 representations of the controls of soil C:N stoichiometry. Importantly, other global changes, such  
606 as changes in temperature and moisture, land use change, and increases in wildfire occurrence  
607 and severity, will likely influence soil C:N differently under the foundational versus emerging  
608 representations but we focus on elevated CO<sub>2</sub> and N deposition here for brevity (Sistla et al.  
609 2014, Pellegrini et al. 2018, Sun et al. 2021).

## 610 4.1 Elevated CO<sub>2</sub>

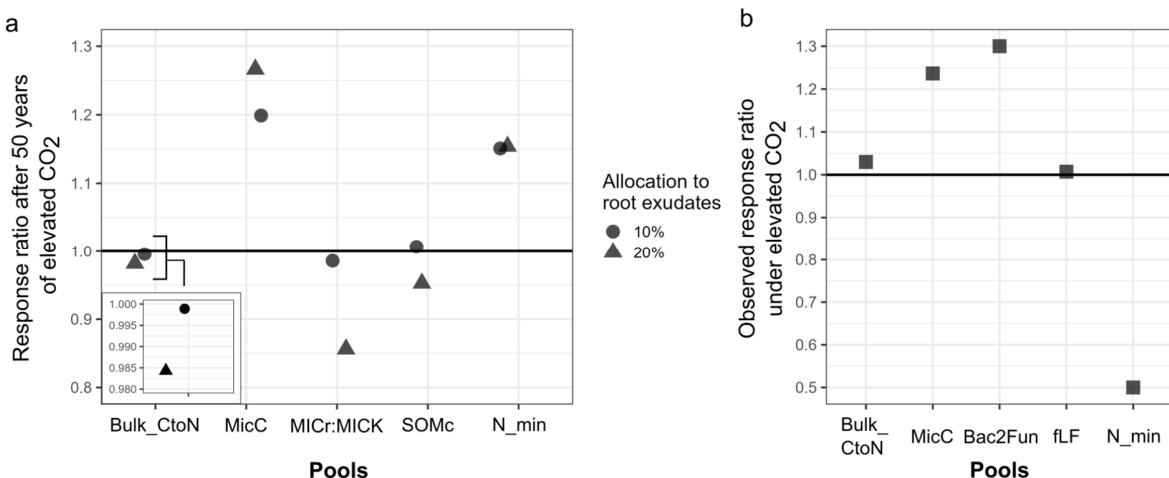
611 As atmospheric CO<sub>2</sub> rises, plant tissue C:N ratios typically increase (Cotrufo et al. 1998,  
612 Wang et al. 2021, Gojon et al. 2022), altering the chemistry of litter inputs to the soil system.  
613 Higher litterfall C:N ratios appear to reduce decomposition rates and soil N availability, possibly  
614 inducing progressive N limitation of vegetation growth (Luo et al. 2004, Liang et al. 2016, Craine  
615 et al. 2018, Mason et al. 2022). Simultaneously, under elevated CO<sub>2</sub> plants can shift allocation  
616 patterns to potentially mitigate N limitation (Phillips et al. 2009). To increase N uptake, plants  
617 increase C allocation to roots and root exudates that both directly enhance plant nutrient  
618 access, while also stimulating soil microbial activity that mineralizes nutrients (Phillips et al.  
619 2011, Cheng et al. 2012, Terrer et al. 2016). Both litter chemistry and plant C allocation changes  
620 under elevated CO<sub>2</sub> could increase soil C:N through greater incorporation of high C:N plant  
621 material and N mining from N-rich SOM, respectively (De Graaf et al. 2006, Phillips et al. 2011).  
622 However, N could also be mined from higher C:N SOM pools, like POM, that are more  
623 accessible to microbes, thereby reducing bulk soil C:N (Sulman et al. 2014). Thus, the relative  
624 influence of litter chemistry and root exudation effects on soil C:N are uncertain but likely  
625 important for a better mechanistic understanding of ecosystem responses to elevated CO<sub>2</sub>.

626 However, accurately capturing ecosystem biogeochemical responses to elevated CO<sub>2</sub>  
627 remains challenging for land models (Zaehle et al. 2013, Davies-Barnard et al. 2020, Eastman  
628 et al. 2023, Hauser et al. 2023). Part of this challenge lies in simulating appropriate plant and

629 soil responses to elevated CO<sub>2</sub> and their interactions. To explore potential soil biogeochemical  
630 responses to elevated CO<sub>2</sub> we conducted a series of idealized model experiments with MIMICS-  
631 CN. Building on the steady-state results presented in the biotic case study (section 3.1.5; Figure  
632 4), we ran a series of 50-year transient simulations for the priming treatment under a pair of  
633 elevated CO<sub>2</sub> scenarios. In the first experiment we represented elevated CO<sub>2</sub> as a 20% step  
634 increase in net primary production (NPP) and a 10% increase in litterfall C:N, relative to the  
635 “ambient” conditions under which the models were initialized (Norby et al. 2005, Wang et al.  
636 2021). For the second experiment we repeated these step increases in productivity and litterfall  
637 C:N, but also increased allocation of C to root exudates from 10% to 20% of metabolic litterfall  
638 inputs, without increasing the total amount of inputs, to evaluate the influence of this emerging  
639 driver. For brevity we calculated the response ratio of different soil pools and fluxes simulated  
640 by MIMICS-CN after 50 years under elevated CO<sub>2</sub> divided by their initial “ambient” state.

641 Increased NPP and litterfall C:N were most influential on soil biogeochemistry when  
642 allocation to root exudates also increased, indicating the importance of representing this  
643 emerging driver (Figure 6a). Increased C allocation to exudates increased microbial biomass,  
644 and particularly that of oligotrophs (reduced MICr:MICK). Oligotrophs preferentially decomposed  
645 the high C:N SOMc pool (comparable to POM), thereby slightly reducing bulk soil C:N. Field  
646 manipulations also report increased microbial biomass and negligible changes in bulk soil C:N  
647 responses under elevated CO<sub>2</sub> that are consistent with our model results (Yue et al. 2017, Zou  
648 et al. 2023). However, empirical studies also suggest that under elevated CO<sub>2</sub>, both the ratio of  
649 copiotrophs:oligotrophs and the POM pool increase (Rocci et al. 2021, Sun et al. 2021).  
650 Additionally, N mineralization increased in our experiments under elevated CO<sub>2</sub> (Figure 6a). This  
651 reflects higher rates of litter N inputs (from increased NPP) that occurred with our elevated CO<sub>2</sub>  
652 experiment but runs contrary to what may be expected under progressive N limitation (Luo et al.  
653 2004). Indeed, when we isolated the potential effects of lower litter quality under elevated CO<sub>2</sub>,  
654 MIMICS-CN showed reduced N mineralization rates, as expected from progressive N limitation

655 (Supplementary Figure 1). We also compare our simulations to the observations from the Duke  
 656 free-air CO<sub>2</sub> enrichment (FACE) experiment because this site exhibits the priming responses we  
 657 evaluate here. We note that this is intended to be a more qualitative comparison than a rigorous  
 658 validation, and note that field measurements were derived from distinct studies under different  
 659 periods of elevated CO<sub>2</sub> treatment. We find remarkably similar increases in microbial biomass  
 660 and similar minimal responses of bulk C:N and SOMc (comparable to the free light fraction of  
 661 SOM) as observed values for our 10% allocation simulations (Figure 6b; Lichter et al., 2005,  
 662 Drake et al. 2011). However, as noted above, increased N mineralization and reduced  
 663 copiotroph to oligotroph ratio are opposite to observed decreases in N mineralization from a  
 664 100-day incubation and increases in the bacterial to fungal ratio (somewhat comparable to the  
 665 copiotroph to oligotroph ratio, Figure 6b, Billings and Ziegler, 2005, Feng et al. 2010). Our  
 666 experiments highlight that plant-microbe-mineral interactions, represented by priming via root  
 667 exudates (an emerging driver), provide a more nuanced assessment of soil C:N responses to  
 668 elevated CO<sub>2</sub> but that further investigation is needed to revise structural assumptions or  
 669 parameterization of MIMICS-CN, or other models trying to represent the emerging  
 670 representation of soil C:N under global change.



671  
 672

673       **Figure 6.** (a) MIMICS-CN simulation results showing response ratios after 50 years of elevated CO<sub>2</sub> (year  
674       50/year 1) with either 10% (circles) or 20% (triangles) of metabolic litter inputs allocated to root exudates.  
675       Elevated CO<sub>2</sub> is implemented as a 20% step increase in net primary production (NPP) and a 10% step  
676       increase in litter C:N. Inset shows bulk soil C:N on a finer scale. (b) Observed response ratios to elevated  
677       CO<sub>2</sub> from the Duke FACE experiment with data from Billings and Ziegler (2005), Lichter et al. (2005),  
678       Feng et al. (2010), and Drake et al. (2011). Note different y-axes. Bulk\_CtoN = bulk soil C:N; MicC =  
679       microbial C; MICr:MICk = copiotroph-to-oligotroph ratio; SOMc = chemically stabilized soil organic matter;  
680       Bac2Fun = bacteria-to-fungi ratio; fLF = free light fraction; N\_min = N mineralization.

681       

## 4.2 Nitrogen Deposition

682       While elevated CO<sub>2</sub> drives increases in ecosystem C:N, N deposition, inputs of reactive  
683       forms of inorganic and organic N from the atmosphere to ecosystems, might be hypothesized to  
684       have the opposite effect. However, ecosystem responses to N deposition are complex and  
685       highly variable across broad spatial scales, suggesting N deposition effects might not be so  
686       straightforward (Schlesinger, 2009, Kanakidou et al. 2016). With N deposition, plant biomass  
687       and shoot:root generally increase and plant shoot, root, and litter C:N generally decrease, which  
688       could be expected to favor microbial use of high quality plant material, ultimately favoring  
689       MAOM formation and lower SOM C:N (Yang et al. 2011, Averill and Waring, 2018, Sun et al.  
690       2020, Feng et al. 2022). In contrast, N deposition could also increase SOM C:N through  
691       reduced lignocellulosic enzyme activity, reduced microbial activity via acidification and C  
692       limitation, and reduced strength of mineral-OM bonds (Frey et al. 2004, Frey et al. 2014,  
693       Carrara et al. 2018, Pan et al. 2020, Ning et al. 2021, Feng et al. 2022). These effects could  
694       specifically increase SOM C:N through reduced decomposition of high C:N SOM (Eastman et  
695       al. 2022), reduced N-rich microbial input, and desorption of relatively N-rich OM, respectively.  
696       The diversity of effects from N deposition have made it difficult to predict consistent drivers of  
697       SOM responses to this global change (Averill and Waring, 2018).

698       Unless specifically formulated to do so, models struggle to depict the wide array of  
699       effects of N deposition. For example, most models add N deposition to the mineral N pool, and  
700       simulations generally show increases in plant productivity and consequently microbial activity.

701 However, N deposition generally reduces microbial activity in empirical studies (Zhang et al.  
702 2018). N deposition in models can also modify plant C:N and drive changes in SOM C:N  
703 through the foundational representation of soil C:N controls (Figure 2a; Throop et al. 2004).  
704 However, most models lack the mechanistic representation for specific enzyme responses,  
705 dynamic and influential soil pH, and N-induced changes in sorption, although the MEND model  
706 represents specific enzyme groups (Wang et al. 2022). Eastman et al. (2023) tackled the  
707 challenge of representing empirical outcomes from a 30-year N deposition experiment in a  
708 mixed hardwood forest in two soil biogeochemistry models (MIMICS-CN and CASA-CN)  
709 coupled to the same vegetation model (CASA-CNP). In order to capture empirical responses in  
710 these models, the authors had to modify the vegetation allocation scheme and decay rate of the  
711 SOMc pool (comparable to POM), and even then only the microbially-explicit model (MIMICS-  
712 CN) exhibited increased soil C:N as seen in the empirical comparison (Eastman et al. 2022,  
713 Eastman et al. 2023). Eastman et al. (2023) demonstrate the difficulty of capturing the multitude  
714 of N deposition effects in models and indicate the need to represent plant and microbe  
715 feedbacks in models to capture soil C:N responses to N deposition.

716 Nitrogen is not the only nutrient whose availability will likely be modified by global  
717 change. Phosphorus (P), in particular, might also shape soil C:N in ways associated with the  
718 emerging representation, largely through interactions with C and N (Townsend et al., 2011). For  
719 example, N fixation is limited by P availability, such that changing availability of P could modify  
720 N fixation with implications for soil C:N (Houlton et al. 2008). Alternatively, under P limitation, N  
721 is allocated to production of phosphatase enzymes that break down SOM, potentially causing a  
722 “P-mining” effect that could preferentially breakdown high P MAOM and thus increase soil C:N  
723 (Treseder and Vitousek, 2001, Spohn, 2020). These N-P interactions are exemplified in CASA-  
724 CNP, CLM-CNP and SCAMPS-CNP and could be used to evaluate effects of P addition on soil  
725 C:N (Wang et al. 2010, Yang et al. 2014, Pold et al. 2022). Alternatively, added P could  
726 directly exchange with C on mineral surfaces to reduce MAOM C:N, which could be formulated

727 in models similarly to acid root exudation (Spohn and Schleuss, 2019, Rocci et al. 2022).  
728 Beyond P, experimentally adding potassium and micronutrients slightly increased soil C:N in  
729 globally-distributed grasslands but adding sulfur stoichiometry to a static soil formulation did not  
730 reduce C cycle uncertainty (Buchkowski et al. 2019, Seabloom et al. 2021). Thus , there is  
731 evidence supporting the influence of nutrient interactions on soil C:N, likely through the  
732 emerging drivers. This supports the development of models that represent both the emerging  
733 drivers and elements beyond C and N.

## 734 5. Conclusions

735 Foundational representations of soil C:N controls present in most models of soil  
736 biogeochemistry are insufficient and could be improved via a more complete, emerging  
737 representation of soil C:N controls. These missing emerging controls likely underlie large scale  
738 patterns of soil C:N and will likely allow for better predictions of soil C:N responses to global  
739 environmental change. The emerging representation of the controls of soil C:N illustrates the  
740 tension between simplicity and accurate representation of complex systems in models.  
741 Balancing these factors is critical for projecting future biogeochemical and climate outcomes.  
742 While the emerging drivers presented have strong empirical support in the literature, there are  
743 many other potential additional drivers that can influence soil C:N ratios including  
744 photodegradation, microbial physiology, and soil fauna (Moorhead and Callaghan, 1994, de  
745 Vries et al. 2013, Mooshammer et al. 2014, Chen et al. 2016). Our review of empirical  
746 understanding of the emerging drivers of soil C:N and their representation in models identified  
747 research gaps and contexts where drivers might be particularly important. We also showed that  
748 implementing the emerging drivers can cause distinct responses of soil C:N to global change.  
749 Ultimately, more theoretical, empirical, and modeling studies are needed to establish the relative  
750 importance of these emerging drivers for soil C:N stoichiometry and if and how they should be

751 implemented in models. Specifically, current understanding informs the need for future research  
752 in the following areas:

753 • Evaluate the feedbacks of different representations of N fixation in models and how  
754 these align with empirically expected feedbacks and change soil C:N

755 • With improved representations of N fixation in models, determine impact of increased  
756 fixation on soil C:N under elevated CO<sub>2</sub>

757 • Use modeling to separately resolve litter quality and N mining/mineralization effects of  
758 mycorrhizal fungi on soil C:N

759 • Determine realistic magnitudes of acid root exudation under steady state and global  
760 change conditions and their influence on soil C:N

761 • Increase collection of mineral composition data to further investigate the importance of  
762 pH and metal controls on MAOM, and subsequently bulk soil C:N

763 • Implement aggregation in a coupled C-N model to evaluate the influence on both  
764 biogeochemical cycles

765 • Investigate relative importance of litter quality versus plant allocation under elevated CO<sub>2</sub>  
766 in a coupled plant-soil model and the implications for soil C:N

767 • Determine the computational cost of adding groups of emerging factors to models to  
768 evaluate the feasibility of representing these factors at a global scale

769 **Acknowledgements**

770 We would like to thank artist Elena Hartley/elabarts.com for her illustrations for Figures 1 and 2.  
771 We would also like to thank the editor and reviewers for their helpful comments. The workshop  
772 in which this work was developed was funded by USDA-NIFA 2020-67019-31395 awarded to  
773 WRW. KSR and WRW were supported by the US National Science Foundation (NSF) award  
774 1926413. PBR and KSR were supported by Biological Integration Institutes award NSF-DBI-  
775 2021898 and the Biosciences Initiative at the University of Michigan. PBR was also supported  
776 by NSF Long-Term Ecological Research award DEB-1831944. EPS, ASG, HHM, and WRW  
777 were supported by NSF Arctic Systems Science Awards 2031253 and 2031238. HHM was also

778 supported by the NSF EMERGE Biology Integration Institute, award # 2022070. CC and EH  
779 acknowledge support from an NSF Research Coordination Network grant to investigate nutrient  
780 cycling in terrestrial ecosystems (INCyTE; DEB-1754126).

781 **References**

782 Abramoff, R., Xu, X., Hartman, M., O'Brien, S., Feng, W., Davidson, E., Finzi, A., Moorhead, D.,  
783 Schimel, J., Torn, M., 2018. The Millennial model: in search of measurable pools and  
784 transformations for modeling soil carbon in the new century. *Biogeochemistry* 137, 51-  
785 71.

786 Abramoff, R.Z., Guenet, B., Zhang, H., Georgiou, K., Xu, X., Rossel, R.A.V., Yuan, W., Ciais, P.,  
787 2022. Improved global-scale predictions of soil carbon stocks with Millennial Version 2.  
788 *Soil Biology and Biochemistry* 164, 108466. This issue.

789 Adams, M. A., Turnbull, T. L., Sprent, J. I., & Buchmann, N., 2016. Legumes are different: Leaf  
790 nitrogen, photosynthesis, and water use efficiency. *Proceedings of the National  
791 Academy of Sciences*, 11, 15, 4098-4103.

792 Amorim, H.C., Hurtarte, L.C., Souza, I.F., Zinn, Y.L., 2022. C:N ratios of bulk soils and particle-  
793 size fractions: Global trends and major drivers. *Geoderma* 425, 116026.

794 An, S., Mentler, A., Mayer, H., Blum, W.E., 2010. Soil aggregation, aggregate stability, organic  
795 carbon and nitrogen in different soil aggregate fractions under forest and shrub  
796 vegetation on the Loess Plateau, China. *Catena* 81, 226-233.

797 Asano, M., Wagai, R., Yamaguchi, N., Takeichi, Y., Maeda, M., Suga, H., Takahashi, Y., 2018.  
798 In Search of a binding agent: Nano-scale evidence of preferential carbon associations  
799 with poorly-crystalline mineral phases in physically-stable, clay-sized aggregates. *Soil  
800 Systems* 2, 32.

801 Averill, C., Turner, B.L., Finzi, A.C., 2014. Mycorrhiza-mediated competition between plants and  
802 decomposers drives soil carbon storage. *Nature* 505, 543–545.  
803 doi:10.1038/nature12901

804 Averill, C., Waring, B., 2018. Nitrogen limitation of decomposition and decay: How can it occur?  
805 *Global Change Biology* 24, 1417-1427.

806 Bailey, V.L., Bond-Lamberty, B., DeAngelis, K., Grandy, A.S., Hawkes, C.V., Heckman, K.,  
807 Lajtha, K., Phillips, R.P., Sulman, B.N., Todd-Brown, K.E., 2018. Soil carbon cycling  
808 proxies: Understanding their critical role in predicting climate change feedbacks. *Global  
809 Change Biology* 24, 895-905.

810 Baskaran, P., Hyvönen, R., Berglund, S.L., Clemmensen, K.E., Ågren, G.I., Lindahl, B.D.,  
811 Manzoni, S., 2017. Modelling the influence of ectomycorrhizal decomposition on plant  
812 nutrition and soil carbon sequestration in boreal forest ecosystems. *New Phytologist*,  
813 213: 1452-1465. doi.org/10.1111/nph.14213

814 Berardi, D., Brzostek, E., Blanc-Betés, E., Davison, B., DeLucia, E.H., Hartman, M.D., Kent, J.,  
815 Parton, W.J., Saha, D., Hudiburg, T.W., 2020. 21st-century biogeochemical modeling:  
816 challenges for Century-based models and where do we go from here? *GCB Bioenergy*  
817 12, 774-788.

818 Billings, S., Ziegler, S., 2005. Linking microbial activity and soil organic matter transformations in  
819 forest soils under elevated CO<sub>2</sub>. *Global Change Biology* 11, 203-212.

820 Blankinship, J.C., Berhe, A.A., Crow, S.E., Druhan, J.L., Heckman, K.A., Keiluweit, M.,  
821 Lawrence, C.R., Marín-Spiotta, E., Plante, A.F., Rasmussen, C., Schadel, C., Schimel,  
822 J.P., Sierra, C. A., Thompson, A., Wagai, R., Wieder, W. R. 2018. Improving

823 understanding of soil organic matter dynamics by triangulating theories, measurements,  
824 and models. *Biogeochemistry* 140, 1-13.

825 Bonan, G.B., Hartman, M.D., Parton, W.J., Wieder, W.R., 2013. Evaluating litter decomposition  
826 in earth system models with long-term litterbag experiments: an example using the  
827 Community Land Model version 4 (CLM 4). *Global Change Biology* 19, 957-974.

828 Bouskill, N.J., Mekonnen, Z., Zhu, Q., Grant, R., Riley, W.J., 2022. Microbial contribution to  
829 post-fire tundra ecosystem recovery over the 21st century. *Communications Earth &*  
830 *Environment* 3, 26.

831 Brzostek, E.R., Greco, A., Drake, J.E. and Finzi, A.C., 2013. Root carbon inputs to the  
832 rhizosphere stimulate extracellular enzyme activity and increase nitrogen availability in  
833 temperate forest soils. *Biogeochemistry* 115, 65-76. doi: 10.1007/s10533-012-9818-9

834 Buchkowski, R.W., Shaw, A.N., Shi, D., Smith, G.R., Keiser, A.D., 2019. Constraining Carbon  
835 and Nutrient Flows in Soil With Ecological Stoichiometry. *Frontiers in Ecology and*  
836 *Evolution* 7, 382. doi: 10.3389/fevo.2019.00382

837 Calabrese, S., Porporato, A., 2019. Impact of ecohydrological fluctuations on iron-redox cycling.  
838 *Soil Biology and Biochemistry* 133, 188–195. doi:10.1016/j.soilbio.2019.03.013

839 Carrara, J.E., Walter, C.A., Hawkins, J.S., Peterjohn, W.T., Averill, C., Brzostek, E.R., 2018.  
840 Interactions among plants, bacteria, and fungi reduce extracellular enzyme activities  
841 under long-term N fertilization. *Global Change Biology* 24, 2721-2734.

842 Chang, K.-Y., Riley, W. J., Crill, P. M., Grant, R. F., Saleska, S. R. 2020. Hysteretic temperature  
843 sensitivity of wetland CH<sub>4</sub> fluxes explained by substrate availability and microbial  
844 activity. *Biogeosciences* 22, 5849-5860.

845 Chen, R., Senbayram, M., Blagodatsky, S., Myachina, O., Ditttert, K., Lin, X., Blagodatskaya, E.,  
846 Kuzyakov, Y. 2014. Soil C and N availability determine the priming effect: microbial N mining  
847 and stoichiometric decomposition theories. *Global Change Biology* 20, 2356-2367.

848 Chen, M., Parton, W.J., Adair, E.C., Asao, S., Hartman, M.D., Gao, W., 2016. Simulation of the  
849 effects of photodecay on long-term litter decay using DayCent. *Ecosphere* 7, 12,  
850 e01631.

851 Cheng, L., Booker, F.L., Tu, C., Burkey, K.O., Zhou, L., Shew, H.D., Rufty, T.W., Hu, S., 2012.  
852 Arbuscular mycorrhizal fungi increase organic carbon decomposition under elevated  
853 CO<sub>2</sub>. *Science* 337, 1084-1087.

854 Cleveland, C.C., Liptzin, D., 2007. C: N: P stoichiometry in soil: is there a “Redfield ratio” for the  
855 microbial biomass? *Biogeochemistry* 85, 235-252.

856 Cleveland, C.C., Reis, C.R.G., Perakis, S.S., Dynarski, K.A., Batterman, S.A., Crews, T.E., Gei,  
857 M., Gundale, M.J., Menge, D.N.L., Peoples, M.B., Reed, S.C., Salmon, V.G., Soper,  
858 F.M., Taylor, B.N., Turner, M.G., Wurzburger, N. 2022. Cryptic nitrogen fixers: An  
859 important frontier in terrestrial N cycling research. *Ecosystems* 25, 1653-1669.

860 Cotrufo, M.F., Ineson, P., Scott, A., 1998. Elevated CO<sub>2</sub> reduces the nitrogen concentration of  
861 plant tissues. *Global Change Biology* 4, 43-54.

862 Cotrufo, M.F., Wallenstein, M.D., Boot, C.M., Denef, K., Paul, E., 2013. The Microbial Efficiency-  
863 Matrix Stabilization (MEMS) framework integrates plant litter decomposition with soil  
864 organic matter stabilization: do labile plant inputs form stable soil organic matter? *Global*  
865 *Change Biology* 19, 988-995.

866 Cotrufo, M.F., Ranalli, M.G., Haddix, M.L., Six, J., Lugato, E., 2019. Soil carbon storage  
867 informed by particulate and mineral-associated organic matter. *Nature Geoscience* 12,  
868 12, 989-994.

869 Craine, J.M., Elmore, A.J., Wang, L., Aranibar, J., Bauters, M., Boeckx, P., Crowley, B.E.,  
870 Dawes, M.A., Delzon, S., Fajardo, A., 2018. Isotopic evidence for oligotrophication of  
871 terrestrial ecosystems. *Nature Ecology & Evolution* 2, 1735-1744.

872 Daly, A.B., Jilling, A., Bowles, T.M., Buchkowski, R.W., Frey, S.D., Kallenbach, C.M., Keiluweit,  
873 M., Mooshammer, M., Schimel, J.P., Grandy, A.S., 2021. A holistic framework

874 integrating plant-microbe-mineral regulation of soil bioavailable nitrogen.  
 875 Biogeochemistry 154, 211-229.

876 Davies-Barnard, T., Friedlingstein, P., 2020. The global distribution of biological nitrogen fixation  
 877 in terrestrial natural ecosystems. *Global Biogeochemical Cycles* 34, 3.

878 Davies-Barnard, T., Meyerholt, J., Zaehle, S., Friedlingstein, P., Brovkin, V., Fan, Y., Fisher,  
 879 R.A., Jones, C.D., Lee, H., Peano, D., 2020. Nitrogen cycling in CMIP6 land surface  
 880 models: progress and limitations. *Biogeosciences* 17, 5129-5148.

881 De Graaff, M.-A., Van Groenigen, K.J., Six, J., Hungate, B., van Kessel, C., 2006. Interactions  
 882 between plant growth and soil nutrient cycling under elevated CO<sub>2</sub>: a meta-analysis.  
 883 *Global Change Biology* 12, 2077-2091.

884 de Vries, F. T., Thébault, E., Liiri, M., Birkhofer, K., Tsiafouli, M. A., Bjørnlund, L., Bracht  
 885 Jørgensen, H., Brady, M. V., Christensen, S., De Ruiter, P., d'Hertefeld, T., Frouz, J.,  
 886 Hedlund, K., Hemerik, L., Hol, W. H. G., Hotes, S., Mortimer, S. R., Setälä, H., Sgardelis,  
 887 S. P., Uteseny, K., Van der Putten, W. H., Wolters, V., and Bardgett, R. D., 2013. Soil  
 888 food web properties explain ecosystem services across European land use systems.  
 889 *Proceedings of the National Academy of Sciences* 110, 14296-14301.

890 Drake, J.E., Gallet-Budynek, A., Hofmockel, K.S., Bernhardt, E.S., Billings, S.A., Jackson, R.B.,  
 891 Johnsen, K.S., Lichter, J., McCarthy, H.R., McCormack, M.L., 2011. Increases in the flux  
 892 of carbon belowground stimulate nitrogen uptake and sustain the long-term  
 893 enhancement of forest productivity under elevated CO<sub>2</sub>. *Ecology Letters* 14, 349-357.

894 Dynarski, K.A., Soper, F.M., Reed, S.C., Wieder, W.R., Cleveland, C.C., 2023. Patterns and  
 895 controls of foliar nutrient stoichiometry and flexibility across United States forests.  
 896 *Ecology* 104, e3909.

897 Eastman, B.A., Adams, M.B., Peterjohn, W.T., 2022. The path less taken: Long-term N  
 898 additions slow leaf litter decomposition and favor the physical transfer pathway of soil  
 899 organic matter formation. *Soil Biology and Biochemistry* 166, 108567.

900 Eastman, B.A., Wieder, W.R., Hartman, M.D., Brzostek, E.R., Peterjohn, W.T., 2023. Can  
 901 models adequately reflect how long-term nitrogen enrichment alters the forest soil  
 902 carbon cycle? *Biogeosciences Discussions*, preprint.

903 Elliott, E.T., 1986. Aggregate Structure and Carbon, Nitrogen, and Phosphorous in Native and  
 904 Cultivated Soils. *Soil Science Society of America Journal* 50, 627-33.

905 Elser, J.J., Sterner, R.W., Gorokhova, E., Fagan, W.F., Markow, T.A., Cotner, J.B., Harrison,  
 906 J.F., Hobbie, S.E., Odell, G.M., Weider, L.W., 2000. Biological stoichiometry from genes  
 907 to ecosystems. *Ecology Letters* 3, 540-550.

908 Elser, J.J., Urabe, J., 1999. The stoichiometry of consumer-driven nutrient recycling: theory,  
 909 observations, and consequences. *Ecology* 80, 735-751.

910 Enríquez, S., Duarte, C.M., Sand-Jensen, K., 1993. Patterns in decomposition rates among  
 911 photosynthetic organisms: the importance of detritus C: N: P content. *Oecologia* 94, 457-  
 912 471.

913 Feng, H., Guo, J., Peng, C., Kneeshaw, D., Roberge, G., Pan, C., Ma, X., Zhou, D., Wang, W.,  
 914 2023. Nitrogen addition promotes terrestrial plants to allocate more biomass to  
 915 aboveground organs: A global meta-analysis. *Global Change Biology* 29, 14, 3970-3989.

916 Feng, X., Simpson, A.J., Schlesinger, W.H., Simpson, M.J., 2010. Altered microbial community  
 917 structure and organic matter composition under elevated CO<sub>2</sub> and N fertilization in the  
 918 duke forest. *Global Change Biology* 16, 2104-2116.

919 Feng, X., Qin, S., Zhang, D., Chen, P., Hu, J., Wang, G., Liu, Y., Wei, B., Li, Q., Yang, Y., 2022.  
 920 Nitrogen input enhances microbial carbon use efficiency by altering plant-microbe-  
 921 mineral interactions. *Global Change Biology* 28, 16, 4845-4860.

922 Fisher, J.B., Sitch, S., Malhi, Y., Fisher, R.A., Huntingford, C. & Tan, S.Y., 2010. Carbon cost of  
 923 plant nitrogen acquisition: a mechanistic, globally applicable model of plant nitrogen  
 924 uptake, retranslocation, and fixation. *Global Biogeochemical Cycles*, 24, 1.

925 Fontaine, S., Mariotti, A., Abbadie, L., 2003. The priming effect of organic matter: a question of  
926 microbial competition? *Soil Biology and Biochemistry* 35, 837-843.

927 Fonte, S.J., Kong, A.Y., van Kessel, C., Hendrix, P.F., Six, J., 2007. Influence of earthworm  
928 activity on aggregate-associated carbon and nitrogen dynamics differs with  
929 agroecosystem management. *Soil Biology and Biochemistry* 39, 1014-1022.

930 Frey, S.D., Knorr, M., Parrent, J.L., Simpson, R.T., 2004. Chronic nitrogen enrichment affects  
931 the structure and function of the soil microbial community in temperate hardwood and  
932 pine forests. *Forest Ecology and Management* 196, 159-171.

933 Frey, S.D., Ollinger, S., Nadelhoffer, K., Bowden, R., Brzostek, E., Burton, A., Caldwell, B.A.,  
934 Crow, S., Goodale, C.L., Grandy, A.S., Finzi, A., Kramer, M.G., Lajtha, K., Lemoine, J.,  
935 Martin, M., McDowell, W.H., Minocha, R., Sadowsky, J.J., Templer, P.H., Wickings, K.,  
936 2014. Chronic nitrogen additions suppress decomposition and sequester soil carbon in  
937 temperate forests. *Biogeochemistry Letters* 121, 305-316.

938 Fulton-Smith, S., Cotrufo, M.F., 2019. Pathways of soil organic matter formation from above and  
939 belowground inputs in a Sorghum bicolor bioenergy crop. *GCB Bioenergy* 11, 971-987.

940 Gao, D., Bai, E., Yang, Y., Zong, S., Hagedorn, F., 2021. A global meta-analysis on freeze-thaw  
941 effects on soil carbon and phosphorus cycling. *Soil Biology and Biochemistry* 159,  
942 108283. <https://doi.org/10.1016/j.soilbio.2021.108283>

943 Georgiou, K., Jackson, R.B., Vinodusková, O., Abramoff, R.Z., Ahlström, A., Feng, W., Frouz, J.,  
944 Harden, J.W., Pellegrini, A.F., Polley, H.W., Soong, J.L., Riley, W.J., Torn, M.S., 2022a.  
945 Synthesis data for manuscript: Global stocks and capacity of mineral-associated soil  
946 organic carbon [Data set]. In *Nature Communications* (v1.0). Zenodo.  
947 <https://doi.org/10.5281/zenodo.5987415>

948 Georgiou, K., Jackson, R.B., Vinodusková, O., Abramoff, R.Z., Ahlström, A., Feng, W., Harden,  
949 J.W., Pellegrini, A.F., Polley, H.W., Soong, J.L., 2022b. Global stocks and capacity of  
950 mineral-associated soil organic carbon. *Nature Communications* 13, 1-12.

951 Georgiou, K., Malhotra, A., Wieder, W.R., Ennis, J.H., Hartman, M.D., Sulman, B.N., Berhe,  
952 A.A., Grandy, A.S., Kyker-Snowman, E., Lajtha, K., 2021. Divergent controls of soil  
953 organic carbon between observations and process-based models. *Biogeochemistry* 156,  
954 5-17.

955 Geyer, K., Schnecker, J., Grandy, A.S., Richter, A., Frey, S., 2020. Assessing microbial  
956 residues in soil as a potential carbon sink and moderator of carbon use efficiency.  
957 *Biogeochemistry* 151, 237-249.

958 Gojon, A., Cassan, O., Bach, L., Lejay, L. & Martin, A. 2022. The decline of plant mineral  
959 nutrition under rising CO<sub>2</sub>: physiological and molecular aspects of a bad deal. *Trends  
960 Plant Sci.* doi:10.1016/j.tplants.2022.09.002

961 Gou, X., Reich, P.B., Qiu, L., Shao, M., Wei, G., Wang, J., Wei, X., 2023. Leguminous plants  
962 significantly increase soil nitrogen cycling across global climates and ecosystem types.  
963 *Global Change Biology* 29, 14.

964 Graf, F., and Frei, M., 2013. Soil Aggregate Stability Related to Soil Density, Root Length, and  
965 Mycorrhiza Using Site-Specific *Alnus Incana* and *Melanogaster Variegatus* s.l.  
966 *Ecological Engineering* 57, 314-323.

967 Grandy, A. S., & Robertson, G. P., 2007. Land-Use Intensity Effects on Soil Organic Carbon  
968 Accumulation Rates and Mechanisms. *Ecosystems* 10, 1, 59–74.  
969 <https://doi.org/10.1007/s10021-006-9010-y>

970 Grandy, A.S., Neff, J.C., Weintraub, M.N., 2007. Carbon structure and enzyme activities in  
971 alpine and forest ecosystems. *Soil Biology and Biochemistry* 39, 2701-2711.

972 Grant, R., Baldocchi, D., Ma, S., 2012. Ecological controls on net ecosystem productivity of a  
973 seasonally dry annual grassland under current and future climates: Modelling with  
974 ecosys. *Agricultural and Forest Meteorology* 152, 189-200.

975 Grant, R.F., Neftel, A., Calanca, P., 2016. Ecological controls on N<sub>2</sub>O emission in surface litter  
976 and near-surface soil of a managed grassland: modelling and measurements.  
977 *Biogeosciences* 13, 3549-3571.

978 Guenet, B., Moyano, F. E., Peylin, P., Ciais, P., Janssens, I. A. 2016. Towards a representation  
979 of priming on soil carbon decomposition in the global land biosphere model ORCHIDEE  
980 (version 1.9.5.2). *Geoscientific Model Development* 9, 841–855. doi.org/10.5194/gmd-9-  
981 841-2016

982 Haddix, M.L., Paul, E.A., Cotrufo, M.F., 2016. Dual, differential isotope labeling shows the  
983 preferential movement of labile plant constituents into mineral-bonded soil organic  
984 matter. *Global Change Biology* 22, 2301-2312.

985 Haddix, M.L., Gregorich, E.G., Helgason, B.L., Janzen, H., Ellert, B.H., Cotrufo, M.F., 2020.  
986 Climate, carbon content, and soil texture control the independent formation and  
987 persistence of particulate and mineral-associated organic matter in soil. *Geoderma* 363,  
988 114160.

989 Hauser E., Wieder, W.R., Bonan, G.B., Cleveland, C.C., 2023. Flexible foliar stoichiometry  
990 reduces the magnitude of the global land carbon sink. *Geophysical Research Letters*  
991 [preprint available through ESSOAR] doi: 10.22541/essoar.168167164.40732205/v1. In  
992 press.

993 He, H., Meyer, A., Jansson, P. E., Svensson, M., Rütting, T., Klemmedsson, L. 2018. Simulating  
994 ectomycorrhiza in boreal forests: implementing ectomycorrhizal fungi model MYCOFON  
995 in CoupModel (v5). *Geoscientific Model Development* 11, 725-751.  
996 doi.org/10.5194/gmd-11-725-2018

997 Hicks, L. C., Leizeaga, A., Rousk, K., Michelsen, A., Rousk, J.. 2020. Simulated rhizosphere  
998 deposits induce microbial N-mining that may accelerate shrubification in the subarctic.  
999 *Ecology* 101, 9, e03094. 10.1002/ecy.3094

1000 Houlton, B.Z., Wang, Y.-P., Vitousek, P.M., Field, C.B., 2008. A unifying framework for  
1001 dinitrogen fixation in the terrestrial biosphere. *Nature* 454, 327-330.

1002 Huang, W., van Bodegom, P. M., Viskari, T., Liski, J., Soudzilovskaia, N. A., 2022.  
1003 Implementation of mycorrhizal mechanisms into soil carbon model improves the  
1004 prediction of long-term processes of plant litter decomposition. *Biogeosciences* 19,  
1005 1469–1490. doi.org/10.5194/bg-19-1469-2022

1006 Hungate, B.A., Van Groenigen, K.J., Six, J., Jastrow, J.D., Luo, Y., De Graaff, M.A., van Kessel,  
1007 C., Osenberg, C.W., 2009. Assessing the effect of elevated carbon dioxide on soil  
1008 carbon: a comparison of four meta-analyses. *Global Change Biology* 15, 2020-2034.

1009 Jilling, A., Keiluweit, M., Contosta, A.R., Frey, S., Schimel, J., Schnecker, J., Smith, R.G.,  
1010 Tiemann, L., Grandy, A.S., 2018. Minerals in the rhizosphere: overlooked mediators of  
1011 soil nitrogen availability to plants and microbes. *Biogeochemistry* 139, 103–122.  
1012 doi:10.1007/s10533-018-0459-5

1013 Jilling, A., Keiluweit, M., Gutknecht, J., Grandy, A.S., 2021. Priming Mechanisms Providing  
1014 Plants And Microbes Access To Mineral-Associated Organic Matter. *Soil Biology and*  
1015 *Biochemistry*, 108265.

1016 Johnson, D.W., Curtis, P.S., 2001. Effects of forest management on soil C and N storage: meta  
1017 analysis. *Forest Ecology and Management* 140, 227-238.

1018 Juice, S.M., Ridgeway, J. R., Hartman M.D., Parton, W. J., Berardi D.M., Sulman, B.N., Allen,  
1019 K.E., and Brzostek, E.R. In review. Reparameterizing litter decomposition using a  
1020 simplified Monte Carlo method improves litter decay simulated by a microbial model and  
1021 alters bioenergy soil carbon estimates.

1022 Kaiser, K., Zech, W., 2000. Sorption of dissolved organic nitrogen by acid subsoil horizons and  
1023 individual mineral phases. *Eur J Soil Sci* 51:403–411.  
1024 https://doi.org/10.1046/j.13652389.2000.00320.x

1025 Kallenbach, C.M., Frey, S.D., Grandy, A.S., 2016. Direct evidence for microbial-derived soil  
1026 organic matter formation and its ecophysiological controls. *Nature Communications* 7,  
1027 13630.

1028 Kanakidou, M., Myriokefalitakis, S., Daskalakis, N., Fanourgakis, G., Nenes, A., Baker, A.,  
1029 Tsigaridis, K., Mihalopoulos, N., 2016. Past, present, and future atmospheric nitrogen  
1030 deposition. *Journal of the Atmospheric Sciences* 73, 2039-2047.

1031 Keiluweit, M., Bougoure, J.J., Nico, P.S., Pett-Ridge, J., Weber, P.K., Kleber, M., 2015. Mineral  
1032 protection of soil carbon counteracted by root exudates. *Nature Climate Change* 5, 588-  
1033 595.

1034 Kleber, M., Mikutta, R., Torn, M.S., Jahn, R. 2005. Poorly crystalline mineral phases protect  
1035 organic matter in acid subsoil horizons. *Eur J Soil Sci* 56, 717-725. <https://doi.org/10.1111/j.1365-2389.2005.00706.x>

1036 Kramer, M.G., Lajtha, K., Aufdenkampe, A.K., 2017. Depth trends of soil organic matter C: N  
1037 and <sup>15</sup>N natural abundance controlled by association with minerals. *Biogeochemistry*  
1038 136, 237-248.

1040 Kou-Giesbrecht, S., Malyshev, S., Martínez Cano, I., Pacala, S.W., Sheviakova, E.,  
1041 Bytnerowicz, T.A., Menge, D.N., 2021. A novel representation of biological nitrogen  
1042 fixation and competitive dynamics between nitrogen-fixing and non-fixing plants in a land  
1043 model (GFDL LM4. 1-BNF). *Biogeosciences* 18, 4143-4183.

1044 Kou-Giesbrecht, S., Arora, V., Seiler, C., Arneth, A., Falk, S., Jain, A., Joos, F., Kennedy, D.,  
1045 Knauer, J., Sitch, S., 2023. Evaluating nitrogen cycling in terrestrial biosphere models:  
1046 Implications for the future terrestrial carbon sink. *Earth System Dynamics* 14, 767-795.

1047 Kyker-Snowman, E., Wieder, W.R., Frey, S.D., Grandy, A.S., 2020. Stoichiometrically coupled  
1048 carbon and nitrogen cycling in the Microbial-MIneral Carbon Stabilization model version  
1049 1.0 (MIMICS-CN v1. 0). *Geoscientific Model Development* 13, 4413-4434.

1050 Lavallee, J.M., Soong, J.L., Cotrufo, M.F., 2020. Conceptualizing soil organic matter into  
1051 particulate and mineral-associated forms to address global change in the 21st century.  
1052 *Global Change Biology* 26, 261–273. doi:10.1111/gcb.14859

1053 Lehmann, J., Kleber, M., 2015. The contentious nature of soil organic matter. *Nature* 528, 60–  
1054 68.

1055 Lehmann, A., Zheng, W., Ryo, M., Soutschek, K., Roy, J., Rongstock, R., Maaß, S., Rillig, M.C.,  
1056 2020. Fungal traits important for soil aggregation. *Frontiers in microbiology* 10, 2904.

1057 Leuthold, S.J., Haddix, M.L., Lavallee, J., Cotrufo, M.F., 2022. Physical fractionation techniques,  
1058 Reference Module in Earth Systems and Environmental Sciences, Elsevier, ISBN  
1059 9780124095489, <https://doi.org/10.1016/B978-0-12-822974-3.00067-7>.

1060 Liang, J., Qi, X., Souza, L., & Luo, Y., 2016. Processes regulating progressive nitrogen limitation  
1061 under elevated carbon dioxide: a meta-analysis. *Biogeosciences* 13, 9, 2689-2699.

1062 Liao, C., Peng, R., Luo, Y., Zhou, X., Wu, X., Fang, C., Chen, J., Li, B., 2008. Altered  
1063 ecosystem carbon and nitrogen cycles by plant invasion: a meta-analysis. *New  
1064 Phytologist* 177, 706-714.

1065 Lichter, J., Barron, S.H., Bevacqua, C.E., Finzi, A.C., Irving, K.F., Stemmler, E.A., Schlesinger,  
1066 W.H., 2005. Soil carbon sequestration and turnover in a pine forest after six years of  
1067 atmospheric CO<sub>2</sub> enrichment. *Ecology* 86, 1835-1847.

1068 Luo, Y., Su, B. O., Currie, W. S., Dukes, J. S., Finzi, A., Hartwig, U., Hungate, B., McMurtrie,  
1069 R.E., Oren, R., Parton, W.J., Pataki, D.E., Shaw, R.M., Zak, D.R., Field, C. B., 2004.  
1070 Progressive nitrogen limitation of ecosystem responses to rising atmospheric carbon  
1071 dioxide. *Bioscience* 54, 8, 731-739.

1072 Luo, Z., Wang, E., Fillery, I.R., Macdonald, L.M., Huth, N., Baldock, J., 2014. Modelling soil  
1073 carbon and nitrogen dynamics using measurable and conceptual soil organic matter  
1074 pools in APSIM. *Agriculture, Ecosystems & Environment* 186, 94-104.

1075 Maaß, S., Caruso, T., Rillig, M.C., 2015. Functional role of microarthropods in soil aggregation.  
1076 *Pedobiologia* 58, 59-63.

1077 Maggi, F., Gu, C., Riley, W.J., Hornberger, G.M., Venterea, R.T., Xu, T., Spycher, N., Steefel, C., Miller, N.L., Oldenburg, C.M., 2008. A mechanistic treatment of the dominant soil  
1078 nitrogen cycling processes: Model development, testing, and application. *Journal of  
1079 Geophysical Research-Biogeosciences* 113.

1080 Mason, R. E., Craine, J. M., Lany, N. K., Jonard, M., Ollinger, S. V., Groffman, P. M., Fulweiler, R.W., Angerer, J., Read, Q.D., Reich, R.B., Templer, P.H., Elmore, A. J., 2022.  
1081 Evidence, causes, and consequences of declining nitrogen availability in terrestrial  
1082 ecosystems. *Science* 376, 6590, eabh3767.

1083 Mekonnen, Z.A., Riley, W.J., Randerson, J.T., Grant, R.F., Rogers, B.M., 2019. Expansion of  
1084 high-latitude deciduous forests driven by interactions between climate warming and fire.  
1085 *Nature Plants* 5, 952-958.

1086 Melillo, J.M., Aber, J.D., Muratore, J.F., 1982. Nitrogen and lignin control of hardwood leaf litter  
1087 decomposition dynamics. *Ecology* 63, 621-626.

1088 Meyerholt, J., Zaehle, S., Smith, M. J., 2016. Variability of projected terrestrial biosphere  
1089 responses to elevated levels of atmospheric CO<sub>2</sub> due to uncertainty in biological  
1090 nitrogen fixation. *Biogeosciences* 13, 5, 1491-1518. doi: 10.5194/bg-13-1491-2016.

1091 Midgley, M.G., Phillips, R.P., 2016. Resource stoichiometry and the biogeochemical  
1092 consequences of nitrogen deposition in a mixed deciduous forest. *Ecology* 97, 3369–  
1093 3377. doi:10.1002/ecy.1595

1094 Mikutta, R., Kaiser, K., Dorr, N., Vollmer, A., Chadwick, O.A., Chorover, J., Kramer, M.G.,  
1095 Guggenberger, G., 2010. Mineralogical impact on organic nitrogen across a long-term  
1096 soil chronosequence (0.3–4100 kyr). *Geochim Cosmochim Acta* 74, 2142–2164.  
1097 <https://doi.org/10.1016/j.gca.2010.01.006>

1098 Mikutta, R., Turner, S., Schippers, A., Gentsc, N., Meyer, S., Condron, L.M., Peltzer, D.A.,  
1099 Richardson, S.J., Eger, A., Hempel, G., Kaiser, K., Klotzbücher, T., Guggenberger, G.,  
1100 2019. Microbial and abiotic controls on mineral-associated organic matter in soil profiles  
1101 along an ecosystem gradient. *Scientific Reports* 9, 1-9.

1102 Moorhead, D.L., Callaghan, T., 1994. Effects of increasing ultraviolet B radiation on  
1103 decomposition and soil organic matter dynamics: a synthesis and modelling study.  
1104 *Biology and Fertility of Soils* 18, 19-26.

1105 Mooshammer, M., Wanek, W., Zechmeister-Boltenstern, S., Richter, A., 2014. Stoichiometric  
1106 imbalances between terrestrial decomposer communities and their resources:  
1107 Mechanisms and implications of microbial adaptations to their resources. *Frontiers in  
1108 Microbiology* 5, 1–10. doi:10.3389/fmicb.2014.00022

1109  
1110 Na, M., Yuan, M., Hicks, L.C., Rousk, J., 2022. Testing the environmental controls of microbial  
1111 nitrogen-mining induced by semi-continuous labile carbon additions in the subarctic. *Soil  
1112 Biology and Biochemistry* 166, 108562.

1113 Nasto, M.K., Winter, K., Turner, B.L., Cleveland, C.C., 2019. Nutrient acquisition strategies  
1114 augment growth in tropical N<sub>2</sub>-fixing trees in nutrient-poor soil and under elevated CO<sub>2</sub>.  
1115 *Ecology* 100, e02646.

1116 NEON (National Ecological Observatory Network). Litterfall and fine woody debris production  
1117 and chemistry (DP1.10033.001), RELEASE-2023. <https://doi.org/10.48443/gf8z-q297>.  
1118 Dataset accessed from <https://data.neonscience.org> on June 2, 2023.

1119 NEON (National Ecological Observatory Network). Root biomass and chemistry, periodic  
1120 (DP1.10067.001), RELEASE-2023. <https://doi.org/10.48443/ecq2-af83>. Dataset  
1121 accessed from <https://data.neonscience.org> on June 2, 2023.

1122 Ning, Q., Hättenschwiler, S., Lü, X., Kardol, P., Zhang, Y., Wei, C., Xu, C., Huang, J., Li, A.,  
1123 Yang, J., 2021. Carbon limitation overrides acidification in mediating soil microbial  
1124

1125 activity to nitrogen enrichment in a temperate grassland. *Global Change Biology* 27, 22,  
1126 5976-5988.

1127 Norby, R. J., DeLucia, E. H., Gielen, B., Calfapietra, C., Giardina, C. P., King, J. S., Ledford, J.,  
1128 McCarthy, H.R., Moore, D.J.P., Ceulemans, R., De Angelis, P., Finzi, A.C., Karnosky,  
1129 D.F., Kubiske, M.E., Lukac, M., Pregitzer, K.S., Scarascia-Mugnozza, G.E., Schlesinger,  
1130 W.H., Oren, R., 2005. Forest response to elevated CO<sub>2</sub> is conserved across a broad  
1131 range of productivity. *Proceedings of the National Academy of Sciences* 102, 50, 18052-  
1132 18056.

1133 Novotny, A. M., Schade, J. D., Hobbie, S. E., Kay, A. D., Kyle, M., Reich, P. B., Elser, J. J.,  
1134 2007. Stoichiometric response of nitrogen-fixing and non-fixing dicots to manipulations of  
1135 CO<sub>2</sub>, nitrogen, and diversity. *Oecologia* 151, 687-696.

1136 Pan, S., Wang, Y., Qiu, Y., Chen, D., Zhang, L., Ye, C., Guo, H., Zhu, W., Chen, A., Xu, G.,  
1137 Zhang, Y., Bai, Y., Hu, S., 2020. Nitrogen-induced acidification, not N-nutrient,  
1138 dominates suppressive N effects on arbuscular mycorrhizal fungi. *Global Change  
1139 Biology* 26, 11, 6568-6580.

1140 Parton W. J., Ojima D. S., Cole C. V., and Schimel D. S., 1994. A general model for soil organic  
1141 matter dynamics: Sensitivity to litter chemistry, texture and management. In *Quantitative  
1142 Modeling of Soil Forming Processes*, SSSA Special Publication (eds. R. B.Bryant, and  
1143 R. W. Arnold). SSSA, vol. 39, pp. 147-167.

1144 Parton W. J., Scurlock J. M. O., Ojima D. S., Gilmanov T. G., Scholes R. J., Schimel D. S.,  
1145 Kirchner T., Menaut J. C., Seastedt T., Moya E. G., Kamalrut A., and Kinyamario J. I.,  
1146 1993. Observations and modeling of biomass and soil organic matter dynamics for the  
1147 grassland biome worldwide. *Global Biogeochemical Cycles* 7, 4, 785-809.

1148 Parton, W., Silver, W.L., Burke, I.C., Grassens, L., Harmon, M.E., Currie, W.S., King, J.Y.,  
1149 Adair, E.C., Brandt, L.A., Hart, S.C., 2007. Global-scale similarities in nitrogen release  
1150 patterns during long-term decomposition. *Science* 315, 361-364.

1151 Pellegrini, A.F., Ahlström, A., Hobbie, S.E., Reich, P.B., Nieradzik, L.P., Staver, A.C.,  
1152 Scharenbroch, B.C., Jumpponen, A., Anderegg, W.R., Randerson, J.T., 2018. Fire  
1153 frequency drives decadal changes in soil carbon and nitrogen and ecosystem  
1154 productivity. *Nature* 553, 194-198.

1155 Peng, J., Wang, Y. P., Houlton, B. Z., Dan, L., Pak, B., Tang, X., 2020. Global Carbon  
1156 Sequestration Is Highly Sensitive to Model-Based Formulations of Nitrogen Fixation.  
1157 *Global Biogeochemical Cycles* 34, e2019GB006296,  
1158 <https://doi.org/10.1029/2019GB006296>.

1159 Perveen, N., Barot, S., Alvarez, G., Klumpp, K., Martin, R., Rapaport, A., Herfurth, D., Louault,  
1160 F., Fontaine, S., 2014. Priming effect and microbial diversity in ecosystem functioning  
1161 and response to global change: a modeling approach using the SYMPHONY model.  
1162 *Global Change Biology* 20, 1174-1190.

1163 Phillips, R.P., Finzi, A.C., Bernhardt, E.S., 2011. Enhanced root exudation induces microbial  
1164 feedbacks to N cycling in a pine forest under long-term CO<sub>2</sub> fumigation. *Ecology Letters*  
1165 14, 187-194.

1166 Phillips, R. P., Bernhardt, E. S., Schlesinger, W. H., 2009. Elevated CO<sub>2</sub> increases root  
1167 exudation from loblolly pine (*Pinus taeda*) seedlings as an N-mediated response. *Tree  
1168 Physiology* 29, 12, 1513-1523.

1169 Phillips, R.P., Brzostek, E., Midgley, M.G., 2013. The mycorrhizal-associated nutrient economy:  
1170 A new framework for predicting carbon-nutrient couplings in temperate forests. *New  
1171 Phytologist* 199, 1, 41-51. doi:10.1111/nph.12221

1172 Possinger, A.R., Zachman, M.J., Enders, A., Levin, B.D., Muller, D.A., Kourkoutis, L.F.,  
1173 Lehmann, J., 2020. Organo-organic and organo-mineral interfaces in soil at the  
1174 nanometer scale. *Nature Communications* 11, 1-11.

1175 Pold, G., Kwiatkowski, B.L., Rastetter, E.B., Sistla, S.A., 2022. Sporadic P limitation constrains  
1176 microbial growth and facilitates SOM accumulation in the stoichiometrically coupled,  
1177 acclimating microbe–plant–soil model. *Soil Biology and Biochemistry* 165, 108489.

1178 Reed, S. C., Cleveland, C. C., Townsend, A. R., 2011. Functional ecology of free-living nitrogen  
1179 fixation: a contemporary perspective. *Annual Review of Ecology, Evolution, and*  
1180 *Systematics* 42, 489–512.

1181 Rizzo, A., Boano, F., Revelli, R., Ridolfi, L., 2014. Decreasing of methanogenic activity in paddy  
1182 fields via lowering ponding water temperature: A modeling investigation. *Soil Biology and*  
1183 *Biochemistry* 75, 211–222. doi:10.1016/j.soilbio.2014.04.016

1184 Robertson, A.D., Paustian, K., Ogle, S., Wallenstein, M.D., Lugato, E., Cotrufo, M.F., 2019.  
1185 Unifying soil organic matter formation and persistence frameworks: the MEMS model.  
1186 *Biogeosciences* 16, 1225–1248.

1187 Rocci, K.S., Lavallee, J.M., Stewart, C.E., Cotrufo, M.F., 2021. Soil organic carbon response to  
1188 global environmental change depends on its distribution between mineral-associated  
1189 and particulate organic matter: A meta-analysis. *Science of the Total Environment* 793.

1190 Rocci, K.S., Barker, K.S., Seabloom, E.W., Borer, E.T., Hobbie, S.E., Bakker, J.D., MacDougall,  
1191 A.S., McCulley, R.L., Moore, J.L., Raynaud, X., Stevens, C.J., Cotrufo, M.F., 2022.  
1192 Impacts of nutrient addition on soil carbon and nitrogen stoichiometry and stability in  
1193 globally-distributed grasslands. *Biogeochemistry* 159, 353–370.

1194 Sardans, J., Penuelas, J., 2012. The role of plants in the effects of global change on nutrient  
1195 availability and stoichiometry in the plant-soil system. *Plant Physiology* 160, 1741–1761,  
1196 doi:10.1104/pp.112.208785

1197 Schimel, J., 2001. 1.13 - Biogeochemical models: Implicit versus explicit microbiology. In E.-D.  
1198 Schulze, M. Heimann, S. Harrison, E. Holland, J. Lloyd, I. C. Prentice & D. S. Schimel  
1199 (Eds.), *Global biogeochemical cycles in the climate system* (pp. 177–183). San Diego,  
1200 IL: Academic Press.

1201 Schimel, J., 2023. Modeling ecosystem-scale carbon dynamics in soil: The microbial dimension.  
1202 *Soil Biology and Biochemistry* 108948.

1203 Schimel, J.P., Bennett, J., 2004. Nitrogen mineralization: Challenges of a changing paradigm.  
1204 *Ecology* 85, 3, 591–602. doi:10.1890/03-8002

1205 Schlesinger, W.H., 2009. On the fate of anthropogenic nitrogen. *Proceedings of the National*  
1206 *Academy of Sciences* 106, 203–208.

1207 Seabloom, E.W., Adler, P.B., Alberti, J., Bieder, L., Buckley, Y.M., Cadotte, M.W., Collins,  
1208 S.L., Dee, L., Fay, P.A., Firn, J., 2021. Increasing effects of chronic nutrient enrichment  
1209 on plant diversity loss and ecosystem productivity over time. *Ecology* 102, e03218.

1210 Segoli, M., De Gryze, S., Dou, F., Lee, J., Post, W.M., Denef, K., Six, J., 2013. AggModel: A soil  
1211 organic matter model with measurable pools for use in incubation studies. *Ecological*  
1212 *Modelling* 263, 1–9.

1213 Shi, M., Fisher, J.B., Brzostek, E.R. & Phillips, R.P., 2016. Carbon cost of plant nitrogen  
1214 acquisition: global carbon cycle impact from an improved plant nitrogen cycle in the  
1215 *Community Land Model*. *Global Change Biology* 22, 1299–1314.

1216 Sistla, S.A., Rastetter, E.B., Schimel, J.P., 2014. Responses of a tundra system to warming  
1217 using SCAMPS: a stoichiometrically coupled, acclimating microbe–plant–soil model.  
1218 *Ecological Monographs* 84, 151–170.

1219 Six, J., Elliott, E.T., Paustian, K., 2000. Soil Macroaggregate Turnover and Microaggregate  
1220 Formation: A Mechanism for C Sequestration under No-Tillage Agriculture. *Soil Biology*  
1221 & *Biochemistry* 32, 14, 2099–2103. [https://doi.org/10.1016/s0038-0717\(00\)00179-6](https://doi.org/10.1016/s0038-0717(00)00179-6).

1222 Six, J., Frey, S.D., Thiet, R.K., Batten, K.M., 2006. Bacterial and fungal contributions to carbon  
1223 sequestration in agroecosystems. *Soil Science Society of America Journal* 70, 555–569.

1224 Song, X., Liu, X., Liang, G., Li, S., Li, J., Zhang, M., Zheng, F., Ding, W., Wu, X., Wu, H., 2022.  
1225 Positive priming effect explained by microbial nitrogen mining and stoichiometric  
1226 decomposition at different stages. *Soil Biology and Biochemistry*, 108852.

1227 Souza, L.F., Billings, S.A., 2021. Temperature and pH mediate stoichiometric constraints of  
1228 organically derived soil nutrients. *Global Change Biology* 28, 4, 1630-1642.

1229 Spohn, M., 2020. Phosphorus and carbon in soil particle size fractions: A synthesis.  
1230 *Biogeochemistry* 147, 225-242.

1231 Spohn, M., Schleuss, P.-M., 2019. Addition of inorganic phosphorus to soil leads to desorption  
1232 of organic compounds and thus to increased soil respiration. *Soil Biology and*  
1233 *Biochemistry* 130, 220-226.

1234 Sulman, B.N., Brzostek, E.R., Medici, C., Sheviakova, E., Menge, D.N.L., Phillips, R.P., 2017.  
1235 Feedbacks between plant N demand and rhizosphere priming depend on type of  
1236 mycorrhizal association. *Ecology Letters* 20, 1043–1053. doi:10.1111/ele.12802

1237 Sulman, B.N., Phillips, R.P., Oishi, A.C., Sheviakova, E., Pacala, S.W., 2014. Microbe-driven  
1238 turnover offsets mineral-mediated storage of soil carbon under elevated CO<sub>2</sub>. *Nature*  
1239 *Climate Change* 4, 1099-1102.

1240 Sulman, B.N., Sheviakova, E., Brzostek, E.R., Kivlin, S.N., Malyshev, S., Menge, D.N.L.,  
1241 Zhang, X., 2019. Diverse Mycorrhizal Associations Enhance Terrestrial C Storage in a  
1242 Global Model. *Global Biogeochemical Cycles* 33, 501–523. doi:10.1029/2018GB005973

1243 Sulman, B.N., Moore, J.A.M., Abramoff, R., Averill, C., Kivlin, S.N., Georgiou, K., Sridhar, B.,  
1244 Hartman, M.D., Wang, G., Wieder, W., Bradford, M.A., Luo, Y., Mayes, M.A., Morrison,  
1245 E.W., Riley, W., Salazar, A., Schimel, J.P., Tang, J., Classen, A.T., 2018. Multiple  
1246 models and experiments underscore large uncertainty in soil carbon dynamics.  
1247 *Biogeochemistry Letters* 141, 109-123.

1248 Sun, Y., Wang, C., Chen, H. Y. H., Luo, X., Qiu, N., & Ruan, H., 2021. Asymmetric responses of  
1249 terrestrial C:N:P stoichiometry to precipitation change. *Global Ecology and*  
1250 *Biogeography* 30, 8, 1724–1735. <https://doi.org/10.1111/geb.13343>

1251 Sun, Y., Wang, C., Yang, J., Liao, J., Chen, H.Y., Ruan, H., 2021. Elevated CO<sub>2</sub> shifts soil  
1252 microbial communities from K-to r-strategists. *Global Ecology and Biogeography* 30,  
1253 961-972.

1254 Sun, Y., Wang, C., Chen, H.Y., Ruan, H., 2020. Responses of C:N stoichiometry in plants, soil,  
1255 and microorganisms to nitrogen addition. *Plant and Soil* 456, 277-287.

1256 Tedersoo, L., Bahram, M., 2019. Mycorrhizal types differ in ecophysiology and alter plant  
1257 nutrition and soil processes. *Biological Reviews* 94, 1857-1880. doi:10.1111/brv.12538

1258 Terrer, C., Phillips, R. P., Hungate, B. A., Rosende, J., Pett-Ridge, J., Craig, M. E., van  
1259 Groenigen, K. J., Keenan, T. F., Sulman, B. N., Stocker, B. D., Reich, P. B., Pellegrini,  
1260 A. F. A., Pendall, E., Zhang, H., Evans, R. D., Carrillo, Y., Fisher, J. B., Van Sundert, K.,  
1261 Vicca, S., Jackson, R. B., 2021. A trade-off between plant and soil carbon storage under  
1262 elevated CO<sub>2</sub>. *Nature* 591, 7851, 599-603. doi: 10.1038/s41586-021-03306-8.

1263 Terrer, C., Vicca, S., Hungate, B.A., Phillips, R.P., Prentice, I.C., 2016. Mycorrhizal association  
1264 as a primary control of the CO<sub>2</sub> fertilization effect. *Science* 353, 72–74.  
1265 doi:10.1126/science.aaf4610

1266 Terrer, C., Vicca, S., Stocker, B.D., Hungate, B.A., Phillips, R.P., Reich, P.B., Finzi, A.C.,  
1267 Prentice, I.C., 2018. Ecosystem responses to elevated CO<sub>2</sub> governed by plant–soil  
1268 interactions and the cost of nitrogen acquisition. *New Phytologist* 217, 507-522.

1269 Thomas, R.Q., Brookshire, E.N.J., Gerber, S., 2015. Nitrogen limitation on land: How can it  
1270 occur in Earth system models? *Global Change Biology* 21, 1777–1793.  
1271 doi:10.1111/gcb.12813

1272 Thornton P.E., Rosenbloom N.A., 2005. Ecosystem model spin-up: estimating steady state  
1273 conditions in a coupled terrestrial carbon and nitrogen cycle model. *Ecological Modelling*  
1274 189, 25–48.

1275 Throop, H.L., Holland, E.A., Parton, W.J., Ojima, D.S., Keough, C.A., 2004. Effects of nitrogen  
1276 deposition and insect herbivory on patterns of ecosystem-level carbon and nitrogen  
1277 dynamics: results from the CENTURY model. *Global Change Biology* 10, 1092-1105.

1278 Tipping, E., Somerville, C.J., Luster, J., 2016. The C: N: P: S stoichiometry of soil organic  
1279 matter. *Biogeochemistry* 130, 117-131.

1280 Townsend, A.R., Cleveland, C.C., Houlton, B.Z., Alden, C.B., White, J.W., 2011. Multi-element  
1281 regulation of the tropical forest carbon cycle. *Frontiers in Ecology and the Environment*  
1282 9, 9-17.

1283 Treseder, K.K., Vitousek, P.M., 2001. Effects of soil nutrient availability on investment in  
1284 acquisition of N and P in Hawaiian rain forests. *Ecology* 82, 946-954.

1285 Vitousek, P. M., Walker, L. R. 1989. Biological invasion by *Myrica faya* in Hawai'i: plant  
1286 demography, nitrogen fixation, ecosystem effects. *Ecological Monographs* 59, 3, 247-  
1287 265.

1288 Vitousek, P. M., Walker, L. R., Whiteaker, L. D., Mueller-Dombois, D., Matson, P. A., 1987.  
1289 Biological invasion by *Myrica faya* alters ecosystem development in Hawaii. *Science*  
1290 238, 4828, 802-804.

1291 Vitousek, P.M., Menge, D.N.L., Reed, S.C., Cleveland, C.C., 2013. Biological nitrogen fixation:  
1292 rates, patterns and ecological controls in terrestrial ecosystems. *Philosophical  
1293 Transactions of the Royal Society B: Biological Sciences* 368, 1-9.

1294 von Lützow, M., Kögel-Knabner, I., Ekschmitt, K., Flessa, H., Guggenberger, G., Matzner, E.,  
1295 Marschner, B., 2007. SOM fractionation methods: relevance to functional pools and to  
1296 stabilization mechanisms. *Soil Biology and Biochemistry* 39, 2183-2207.

1297 Wang, C., Sun, Y., Chen, H. Y. H., Ruan, H., 2021. Effects of elevated CO<sub>2</sub> on the C:N  
1298 stoichiometry of plants, soils, and microorganisms in terrestrial ecosystems. *Catena* 201.  
1299 doi:10.1016/j.catena.2021.105219.

1300 Wang, G., Gao, Q., Yang, Y., Hobbie, S.E., Reich, P.B., Zhou, J., 2022. Soil enzymes as  
1301 indicators of soil function: A step toward greater realism in microbial ecological modeling.  
1302 *Global Change Biology* 28, 1935-1950.

1303 Wang, Y. P., Law, R. M., Pak, B., 2010. A global model of carbon, nitrogen and phosphorus  
1304 cycles for the terrestrial biosphere. *Biogeosciences* 7, 2261-2282.  
1305 https://doi.org/10.5194/bg-7-2261-2010

1306 Weedon, J.T., Cornwell, W.K., Cornelissen, J.H., Zanne, A.E., Wirth, C., Coomes, D.A., 2009.  
1307 Global meta-analysis of wood decomposition rates: a role for trait variation among tree  
1308 species? *Ecology Letters* 12, 45-56.

1309 Wieder, W.R., Cleveland, C.C., Townsend, A.R., 2009. Controls over leaf litter decomposition in  
1310 wet tropical forests. *Ecology* 90, 3333-3341

1311 Wieder, W., Grandy, A., Kallenbach, C., Bonan, G., 2014. Integrating microbial physiology and  
1312 physio-chemical principles in soils with the Microbial-MIneral Carbon Stabilization  
1313 (MIMICS) model. *Biogeosciences* 11, 3899-3917.

1314 Wieder, W.R., Cleveland, C.C., Lawrence, D.M., Bonan, G.B., 2015. Effects of model structural  
1315 uncertainty on carbon cycle projections: biological nitrogen fixation as a case study.  
1316 *Environmental Research Letters* 10, 044016.

1317 Wieder, W.R., Pierson, D., Earl, S., Lajtha, K., Baer, S.G., Ballantyne, F., Berhe, A.A., Billings,  
1318 S.A., Brigham, L.M., Chacon, S.S., 2021. SoDaH: the SOils DAta Harmonization  
1319 database, an open-source synthesis of soil data from research networks, version 1.0.  
1320 *Earth System Science Data* 13, 1843-1854.

1321 Wieder, W.R., Sulman, B.N., Hartman, M.D., Koven, C.D., Bradford, M.A., 2019a. Arctic soil  
1322 governs whether climate change drives global losses or gains in soil carbon.  
1323 *Geophysical Research Letters* 46, 14486-14495.

1324 Wieder, W. R., Lawrence, D.M., Fisher, R.A., Bonan, G.B., Cheng, S.J., Goodale, C.L., Grandy,  
1325 A.S., Koven, C.D., Lombardozzi, D.L., Oleson, K.W., Thomas, R.Q., 2019b. Beyond

1326 Static Benchmarking: Using Experimental Manipulations to Evaluate Land Model  
 1327 Assumptions. *Global Biogeochemical Cycles* 33, 1289-1309,  
 1328 doi:10.1029/2018GB006141.

1329 Wieder, W.R., Hartman, M.D., Sulman, B.N., Wang, Y.P., Koven, C.D., Bonan, G.B., 2018.  
 1330 Carbon cycle confidence and uncertainty: Exploring variation among soil biogeochemical  
 1331 models. *Global Change Biology* 24, 1563-157

1332 Wookey, P.A., Aerts, R., Bardgett, R.D., Baptist, F., Bråthen, K.A., Cornelissen, J.H., Gough, L.,  
 1333 Hartley, I.P., Hopkins, D.W., Lavorel, S. and Shaver, G.R., 2009. Ecosystem feedbacks  
 1334 and cascade processes: understanding their role in the responses of Arctic and alpine  
 1335 ecosystems to environmental change. *Global Change Biology* 15, 1153-1172.  
 1336 doi.org/10.1111/j.1365-2486.2008.01801.x

1337 Xu, X.F., Thornton, P.E., Post, W.M., 2013. A global analysis of soil microbial biomass carbon,  
 1338 nitrogen and phosphorus in terrestrial ecosystems. *Global Ecology and Biogeography*  
 1339 22, 737-749.

1340 Yang, Y., Luo, Y., Lu, M., Schädel, C., Han, W., 2011. Terrestrial C: N stoichiometry in response  
 1341 to elevated CO<sub>2</sub> and N addition: a synthesis of two meta-analyses. *Plant and Soil* 343,  
 1342 393-400.

1343 Yang, X., Thornton, P., Ricciuto, D., Post, W., 2014. The role of phosphorus dynamics in  
 1344 tropical forests—a modeling study using CLM-CNP. *Biogeosciences* 11, 1667-1681.

1345 Yu, W.H., Li, N., Tong, D.S., Zhou, C.H., Lin, C.X., Xu, C.Y., 2013. Adsorption of proteins and  
 1346 nucleic acids on clay minerals and their interactions: a review. *Appl Clay Sci* 80-81:443-  
 1347 452. https://doi.org/10.1016/j.clay.2013.06.003.

1348 Yue, K., Fornara, D.A., Yang, W., Peng, Y., Li, Z., Wu, F., Peng, C., 2017. Effects of three  
 1349 global change drivers on terrestrial C: N: P stoichiometry: a global synthesis. *Global  
 1350 Change Biology* 23, 2450-2463.

1351 Zaehle, S., Medlyn, B. E., De Kauwe, M. G., Walker, A. P., Dietze, M. C., Hickler, T., Luo, Y.,  
 1352 Wang, Y.-P., El-Masri, B., Thornton, P., Jain, A., Wang, S., Warlind, D., Weng, E.,  
 1353 Parton, W., Iversen, C. M., Gallet-Budynek, A., McCarthy, H., Finzi, A., Hanson, P. J.,  
 1354 Prentice, I. C., Oren, R., Norby, R. J. 2014. Evaluation of 11 terrestrial carbon–nitrogen  
 1355 cycle models against observations from two temperate Free-Air CO<sub>2</sub> Enrichment  
 1356 studies. *New Phytologist* 202, 3, 803-822. doi: 10.1111/nph.12697.

1357 Zhang, J., Elser, J.J., 2017. Carbon: nitrogen: phosphorus stoichiometry in fungi: a meta-  
 1358 analysis. *Frontiers in Microbiology* 8, 1281.

1359 Zhang, T.A., Chen, H.Y., Ruan, H., 2018. Global negative effects of nitrogen deposition on soil  
 1360 microbes. *The ISME journal* 12, 1817.

1361 Zhang, Y., Lavallee, J.M., Robertson, A.D., Even, R., Ogle, S.M., Paustian, K., Cotrufo, M.F.,  
 1362 2021. Simulating measurable ecosystem carbon and nitrogen dynamics with the  
 1363 mechanistically defined MEMS 2.0 model. *Biogeosciences* 18, 3147-3171.

1364 Zhao, Q., Callister, S.J., Thompson, A.M., Kukkadapu, R.K., Tfaily, M.M., Bramer, L.M., Qafoku,  
 1365 N.P., Bell, S.L., Hobbie, S.E., Seabloom, E.W., 2020. Strong mineralogic control of soil  
 1366 organic matter composition in response to nutrient addition across diverse grassland  
 1367 sites. *Science of the Total Environment* 736, 137839.

1368 Zimmermann, M., Leifeld, J., Schmidt, M., Smith, P., Fuhrer, J., 2007. Measured soil organic  
 1369 matter fractions can be related to pools in the RothC model. *European Journal of Soil  
 1370 Science* 58, 658-667.

1371 Zou, J., Zhang, W., Zhang, Y., Wu, J., 2023. Global patterns of plant and microbial biomass in  
 1372 response to CO<sub>2</sub> fumigation. *Frontiers in Microbiology* 14, 1175854.

1373